Atmospheric infrasound generation by ocean waves in finite depth: unified theory and application to radiation patterns

Marine de Carlo, Fabrice Ardhuin, Alexis Le Pichon

Atmospheric infrasound generation by ocean waves in finite depth: unified theory and application to radiation patterns

Article *in* Geophysical Journal International · February 2020

CITATION
1

READS
146

3 authors:

Marine De Carlo
Atomic Energy and Alternative Energies Commission
10 PUBLICATIONS **3** CITATIONS
SEE PROFILE

Fabrice Ardhuin
University of California, San Diego
314 PUBLICATIONS **6,161** CITATIONS
SEE PROFILE

Alexis Le Pichon
225 PUBLICATIONS **2,443** CITATIONS
SEE PROFILE

submitted to *Geophys. J. Int.*

Atmospheric infrasound generation by ocean waves in finite depth: unified theory and application to radiation patterns

M. De Carlo[1, 2], F. Ardhuin[2,3], A. Le Pichon[1]

[1] *CEA, DAM, DIF, F-91297, Arpajon, France;* [2] *Univ. Brest, CNRS, IRD, Ifremer, Laboratoire d'Océanographie Physique et Spatiale (LOPS), IUEM, Brest, France*

[3] *Marine Physical Laboratory, Scripps Institution of Oceanography, La Jolla, CA, USA*

Received XX; in original form 2019 June 10

SUMMARY

Between 0.1 and 0.5 Hz, infrasound signals recorded in the atmosphere are dominated by ocean-generated noise called microbaroms. Microbaroms propagate through the atmosphere over thousands of kilometers due to low absorption and efficient ducting between the ground and the stratopause. Different theoretical models have been developed to characterize the source of microbaroms, all based on the second-order non-linear interaction of ocean waves. While early theories considered an infinite ocean depth and a source radiation depending on the acoustic wave elevation angle, other works have approximated the radiation pattern as a monopole, and found a considerable effect of the water depth. This paper reviews these models and extends the previous theories to the combined effects of both finite depth ocean and source directivity in both elevation and azimuth angles. It is found that the water depth has a negligible effect for the near-horizontally propagating acoustic waves that should dominate the measured microbarom records. Another important result is that the microbarom azimuthal variation can be highly directive locally, but it generally becomes isotropic when integrated over a realistic source region.

Key words: Infrasound – Interface waves – Wave propagation

1 INTRODUCTION

Continuous oscillations of the ground displacement and atmospheric pressure, named respectively secondary microseisms and microbaroms, are measured worldwide by seismological and infrasound networks with a dominant frequency around 0.2 Hz (Benioff & Gutemberg, 1939). They are generated by second-order non linear interaction of ocean gravity waves of similar frequency propagating in almost opposite directions (Longuet-Higgins, 1950; Hasselmann, 1963).

Microbarom propagate through the atmosphere over large distances due to low absorption rates and efficient atmospheric ducting between the ground and the stratopause (Drob, 2019; Waxler & Assink, 2019). Studying microbaroms recorded for four years at Palisades, New York, (Donn & Rind, 1971) have revealed the importance of winds in the higher atmosphere for their propagation, pointing to the capability of ground-based measurements to probe the higher atmosphere, for which very few other observations are available.

Recent developments of infrasound networks at global and continental scales facilitate the analysis of acoustic waves for probing unresolved atmospheric structures in the middle atmosphere (Marty, 2019; Blanc et al., 2018). This has motivated mathematical developments of geophysical inverse problems using infrasound from well identified sources (Drob et al., 2010; Assink et al., 2014). Ducting of infrasound depends on the 3-D wind and temperature fields and is most efficient if the propagation direction coincides with the polar vortex at mid-latitude regions. In particular, the main characteristics of Sudden Stratospheric Warming events have been successfully derived from directional microbarom amplitude variations resulting from changes in stratospheric and thermospheric propagation conditions (e.g. Garcés et al., 2002; Landès et al., 2010; Smets & Evers, 2014). Such studies demonstrate the advantage of an infrastructure that integrates independent middle atmospheric measurement techniques currently not assimilated in numerical weather prediction models (NWP) and provides quantitative understanding of stratosphere-troposphere dynamical coupling useful for NWP applications (Le Pichon et al., 2015).

So far, microbarom studies have used qualitative comparisons between source models and received signals, with sdifficulties of interpretation associated with uncertainties in the measurements and in the propagation. Thanks to novel measurements from a statospheric balloon fitted

with microbarometers, Bowman & Lees (2018) were able to verify quantitatively the predictions based on numerical ocean wave models and the microbarom source theory of Waxler et al. (2007) using measured sound spectra over the Southern Ocean. Their further interpretation of microbaroms as a major heat source for the thermosphere, well above their measurement altitude, relies on the monopolar radiation pattern predicted by Waxler & Gilbert (2006).

Following the work of Longuet-Higgins (1950) on microseisms, a first theory of microbarom generation was proposed by Posmentier (1967), with the atmospheric motion coming from the continuity of the velocity field at the air-sea interface, and no feedback of the atmosphere on the pressure field in the ocean. A more complete theory for random waves, consistent with the microseism generation theory of Hasselmann (1963) and an accurate treatment of the air-sea boundary condition is given by Brekhovskikh et al. (1973), leading to significant differences for near-horizontal propagation. However, that work only considered an ocean of infinite depth. The effect of the ocean depth, with the amplification of particular frequencies corresponding to an 'organ pipe resonance' of the water column, was later considered by Waxler et al. (2007), extending the work done by Waxler & Gilbert (2006).The major difference between that work and the earlier analysis of Brekhovskikh et al. (1973) is the monopole radiation pattern that, as we show here, comes from an assumption on the coherence of the source over only very short scales whereas Brekhovskikh et al. (1973) did not introduce this assumption. A unified theory is thus necessary for further quantitative analysis of microbarom records and the analysis of their impact in regions where no measurement is available, such as the thermosphere.

Given that microbaroms and microseisms are related (Donn & Naini, 1973) it is interesting to discuss microseisms for which more quantitative analyses are available. Microseisms have their most energetic sources assocated to severe ocean storms but not necessarily co-located with the storm due to the propagation of ocean waves as swells (Obrebski et al., 2012). In particular, measurements at seismic stations near coasts can be dominated by the interaction of storm waves with their reflection from the coast (Bromirski et al., 1999; Ardhuin et al., 2011). In general, the sources at a frequency f_s correspond to the interaction of waves with similar frequencies $f = f_s/2$ and nearly opposite directions, as illustrated in Fig. 1.

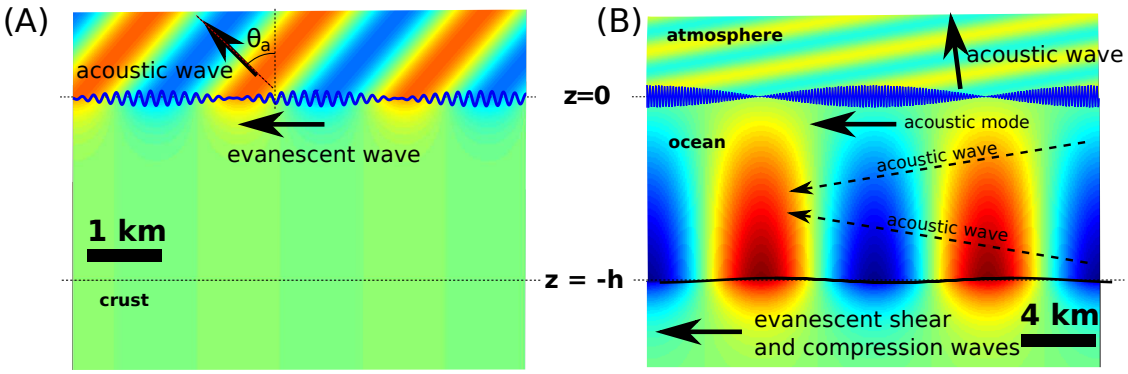

Figure 1. Example of vertical cross-section of the pressure pattern, in colors, radiated by a pair of interacting ocean wave trains of period around 10 s. The sea surface elevation, plotted as a blue line around $z = 0$ is the sum of the elevations of the two wave trains and has a wave group structure. (A) The periods of the two wave trains are 10 s and 9.66 s (B) 10 s and 9.94 s. Note that the vertical displacement of the sea surface is strongly exaggerated in order to make waves visible. A realistic ocean wave field includes many wave trains and thus all possible pairs of interactions radiating acoustic waves in all directions θ_a. As the two periods of the wave train get closer, from (A) to (B), the lengths of the groups get larger and the angle θ_a becomes smaller. This paper focuses on the radiated power as a function of θ_a.

The generation of acoustic and seismic modes in the ocean and solid Earth with horizontal propagation speeds that exceed 1500 m/s, much more than the typical ocean waves phase speeds around 15 m/s, was explained quantitatively by Hasselmann (1963) as the result of an interference of pairs of ocean wave trains of wavenumbers $\mathbf{k}$ and $\mathbf{k}'$, giving seismic or acoustic waves at the wavenumber $\mathbf{K} = \mathbf{k} + \mathbf{k}'$. The microseism generation theory is one particular example of the general theory of wave-wave interactions developed by Hasselmann (1966). The horizontal radiation pattern of a single pair of ocean waves gives a single sinusoidal pressure field propagating in the direction φ_2 of the wavenumber vector $\mathbf{K}$. For microseisms $K = |\mathbf{K}|$ is generally much smaller than the width of the ocean wave spectrum, so that the combination of all pairs of ocean waves gives an isotropic source.

In the case of microbaroms of frequency 0.2 Hz, the sound speed in the air is only 20 times the phase speed of the ocean waves, so that K is comparable to the ocean wave spectrum width, and there may be a preferential radiation in some directions φ_2. Applications and further analysis of microbaroms require a knowledge of the source magnitude and variability. In recent work, Waxler et al. (2007) investigated the influence of the water depth on the source magnitude, similar to what

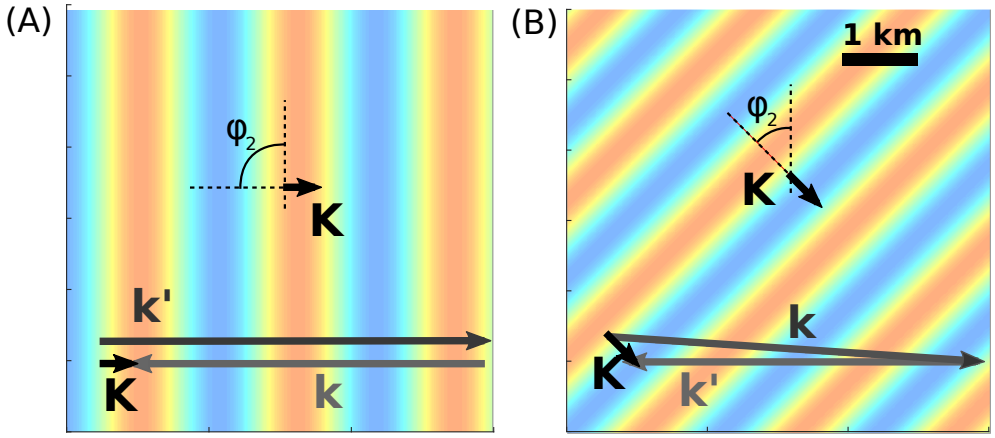

Figure 2. Example of horizontal pressure patterns, in colors, radiated by a pair of interacting ocean wave trains of periods 10 s and 9.66 s with (A) opposing directions (B) not exactly opposing directions. For acoustic waves, the maximum magnitude K of the wavenumber vector $\mathbf{K}$ corresponds to horizontal propagation with $K = \Omega/\alpha_a$ and can be in any azimuth φ_2 depending on the exact ocean wave wavenumbers $\mathbf{k}$ and $\mathbf{k}'$. Modes with larger values of K decay exponentially over the vertical and are not relevant for microbaroms measured on land.

is found for microseisms. The conclusion of the present paper is that the effect of water depth depends on the angle θ_a of the sound propagation relative to the vertical direction, and that the pressure field of microbaroms over the ocean generally contains a wide range of angles. Indeed, the coupling of the ocean and atmosphere strongly depends on θ_a, as demonstrated by Brekhovskikh et al. (1973), but neglected by Waxler & Gilbert (2006).

This importance of θ_a is now well known for microseisms and is easy to understand in relation to the physical properties of the solid Earth, ocean, and atmosphere. A usual approximation of the propagating medium is a stack of uniform horizontal layers l characterized by different velocities of propagation α_l and β_l for compression and shear waves. Close to the source, microseisms are dominated by Rayleigh waves that correspond to relatively slow components, with horizontal propagation speeds between the sound speed in water α_w, and the shear wave speed in the crust β_c. These Rayleigh modes combine motions that decay exponentially with depth in the solid Earth, with propagating acoustic waves in the ocean, and their acoustic propagation angles in the water θ_w are larger than $\arcsin(\alpha_w/\beta_c) \simeq 30°$ (Ardhuin et al., 2019). For very large distances, seismic body waves may dominate the signal because of their weaker attenuation with distance, and these are due to the ocean acoustic noise that is more nearly vertical, allowing propagation in the crust,

with $\theta_w < \arcsin(\alpha_w/\alpha_c) \simeq 16°$. The water depth effect is clearly different for Rayleigh and body waves, as predicted by Ardhuin & Herbers (2013) and Gualtieri et al. (2014), and demonstrated by (Obrebski et al., 2013) and Meschede et al. (2017).

Now looking at microbaroms, we expect similar dependencies on θ_a because different components of the ocean wave forcing field, with wavenumbers $\mathbf{K} = \mathbf{k} + \mathbf{k}'$ give acoustic modes that have different apparent horizontal speeds $C = 2\pi f_s/|\mathbf{K}|$. Speed faster than the compression speed in the crust $C > \alpha_c$ leads to the generation of compression P-waves in the solid Earth, corresponding to nearly vertical propagation in the ocean layer and even more vertical propagation in the atmosphere, given by Snell's law. The limit $C \to \infty$ corresponding to vertical propagation and $|\mathbf{K}| = \mathbf{0}$, which are the exactly standing waves of Longuet-Higgins. At the other extreme, $C < \alpha_w$ gives evanescent waves in the water layer that correspond to acoustic-gravity (AG) modes that dominate the pressure field measured in the top 300 m of the ocean, as observed by Cox & Jacobs (1989) and Ardhuin et al. (2013). For these AG modes, we expect no influence of water depths larger than 300 m on the pressure at the ocean surface. These AG waves are coupled to atmospheric acoustic waves that have propagation angles larger than $\theta_{a0} = \arcsin \alpha_a/\alpha_w \simeq 12°$.

The difference in water depth effects between body waves, Rayleigh waves and AG modes should influence the amplitude of acoustic waves radiated in the atmosphere, and the amplitude of microbaroms should strongly depend on the direction of propagation θ_a relative to the vertical. The decomposition of the ocean wave forcing in different horizontal wavenumbers $\mathbf{K} = K\,(\cos\varphi_2,\ \sin\varphi_2)$ allows to consider separately the different acoustic wave components and how they may contribute to different acoustic modes. Each K corresponds to a propagation angle such that $\sin\theta_l = K\,\alpha_l/(2\pi f_s)$ where α_l is the sound speed in the layer l, which is related to Snell's law.

Because the ocean wave spectra are relatively broad, they contain a wide range of pairs $\mathbf{k}$ and $\mathbf{k}'$ so that all possible $\mathbf{K}$ are excited simultaneously. For microseisms, this produces a spectrum of the excitation that is white in wavenumber, and thus equivalent to a point force. In the case of microbaroms, the conversion from wave motion to acoustic pressure is a function of the wavenumber K, first given by Brekhovskikh et al. (1973), which determines the radiation pattern in the atmosphere.

Hence the previous works either lack the possible important effect of finite depth in the ocean, or important aspects of the radiation pattern in the atmosphere. In order to progress towards a quantitative understanding of microbarom signals it is thus necessary to have both effects in the same theory, and this is the objective of the present paper. For the sake of simplicity, we only consider the case of a homogeneous atmosphere, and extend the theory of Brekhovskikh et al. (1973) to take into account a finite water depth. The theoretical formulation and the main results are given in section 2, with details of the derivation in the Supporting Information. These results are interpreted in section 3 and conclusions follow in section 4.

2 A GENERAL THEORY OF MICROBAROM SOURCES

In order to facilitate the translation between the different papers we have listed in table 1 the correspondence of the main symbols used. We have also included Longuet-Higgins (1950) because it treats almost the same physical problem, with a focus on the water layer, and the same decomposition in particular and homogeneous solutions of the forced wave equation.

As detailed in the Supporting information, which follows the method of Brekhovskikh et al. (1973), the basis of microseism and microbaroms generation theory is the coupling of motions in different layers, with a forcing coming from nonlinear ocean wave effects, in which the nonlinearity is necessary to allow the generation of waves with long wavelenghts $2\pi/|\mathbf{k}+\mathbf{k}'|$ from the interference of shorter ocean waves with wavelengths $2\pi/|\mathbf{k}|$ and $2\pi/|\mathbf{k}|'$. The velocity potential ϕ in layer l is solution of a wave equation (Brekhovskikh et al., 1973),

$$\frac{\partial^2\phi}{\partial t^2} - \alpha_l^2\nabla^2\phi = -\frac{\partial}{\partial t}(\nabla\phi)^2 - g\frac{\partial\phi}{\partial z}, \tag{1}$$

where ∇^2 is the 3-dimensional Laplace operator. The two terms on the right hand side can be neglected in the water layer (Longuet-Higgins, 1950), but are generally significant in the air. The first term corresponds to the effect of compressibility. It adds one particular solution ϕ_p that is zero away from the boundary but modifies the homogeneous solution via the boundary condition at the air-sea interface. The second term is the effect of gravity, which gives a weak additional $\exp(gz/2\alpha_l^2)$ vertical decay, with a half-decay distance of 15 km in the atmosphere and 300 km

Table 1. Notations used in different papers: LH50 stands for Longuet-Higgins (1950), BGKN73 stands for Brekhovskikh et al. (1973), WG06 stands for Waxler & Gilbert (2006) and AH13 stands for Ardhuin & Herbers (2013).

quantity	this paper	LH50	BGKN73	WG06	AH13
vertical coordinate	z	$-z$	z	z	z
angle relative to vertical	θ_a or θ_w	–	θ_1 or θ_2	–	–
surface elevation	ζ	ζ	ζ	ξ	ζ
azimuth of spectrum	φ	θ	φ	θ	θ
azimuth of acoustic signal	φ_2	–	φ_a	–	–
velocity potential	ϕ	$-\phi$	$-\varphi$	ϕ	ϕ
layer index	l	–	j	σ	–
sound speed	α_l	c	c_j	c_σ	α
density ratio	m	–	m	–	–
horizontal wavenumber	$\mathbf{K}$	–	$\mathbf{q}$	–	$\mathbf{K}$
radian frequency	Ω	–	Ω	–	$2\pi f_s$
horizontal wavenumbers	$\mathbf{k}$, $\mathbf{k}'$	$(-uk, -vk)$	$\varkappa$, $\varkappa_1$	$\mathbf{k}$, $\mathbf{q}$	$\mathbf{k}$, $\mathbf{k}'$
radian frequencies	σ, σ'	σ	$\omega(\varkappa)$,$\omega(\varkappa_1)$	$\omega(\mathbf{k})$,$\omega(\mathbf{q})$	σ, σ'
pressure	p	p	$\rho\mathcal{P}$	p	p
vertical wavenumbers	ν , μ	– , α	λ_1,λ_2	–	l_a, l
upward amplification	$g/2\alpha_l$	γ	–	–	–

in the ocean. That second effect was considered by Brekhovskikh et al. (1973) but neglected in Waxler & Gilbert (2006).

Neglecting these two terms for the water layer, solutions that are periodic in time and space take the following homogeneous form, with $\Omega = 2\pi f_s$ the radian frequency and $\kappa_a = \nu_+$ and $\kappa_w = \mu_-$ the vertical wave-numbers (going upwards in the air and downwards in the water)

$$\begin{aligned} \phi &= \sum_{\mathbf{k}} \Phi_l \exp\left[\mathrm{i}\left(\mathbf{K}\cdot\mathbf{x} + \kappa_l z - \Omega t\right)\right] + \text{c.c.} \\ &= \sum_{\mathbf{k},s} \Phi_l \exp\left[\mathrm{i}\left(\mathbf{K}\cdot\mathbf{x} + \kappa_l z - s\Omega t\right)\right], \end{aligned} \tag{2}$$

where c.c. stands for the complex conjugate and $s = 1$ or $s = -1$ is a sign index. Neglecting the right hand side of (1), one gets

$$\kappa_l^2 + K^2 = \Omega^2/\alpha_l^2. \tag{3}$$

With N the number of unknown potential amplitudes $(\Phi_i)_{1\leq i\leq N}$, there are N continuity conditions for stresses and displacements at the layer interfaces, linking the N amplitudes of velocity potentials.

All the variables, the pressure p, the density ρ, the velocity potential ϕ and the sea surface elevation ζ are expanded in powers of $\varepsilon = ak$ that is the product of a typical ocean wave wavenumber k and surface elevation amplitude a,

$$p = p_0 + p_1 + p_2 + ... \tag{4}$$

$$\rho = \rho_0 + \rho_1 + \rho_2 + ... \tag{5}$$

$$\phi = \phi_0 + \phi_1 + \phi_2 + ... \tag{6}$$

$$\zeta = \zeta_0 + \zeta_1 + \zeta_2 + ... \tag{7}$$

In addition to the wave slope ε, two other small parameters are defined, the ratio between the air and water densities $m = \rho_a/\rho_w$ and $\delta_l = \sigma/k\alpha_l$ the ratio between the speed of surface waves and the speed of sound in the air or water.

Collecting the terms of same order, we obtain at each order a system of N equations for N unknowns with a detailed derivation in Supporting Information. At order ε^0, the solution is the hydrostatic equilibrium of pressure and gravity. The first order solution corresponds to Airy waves, which are linear gravity waves, with negligible $O(\delta_w^2)$ and $O(m)$ corrections due to the presence of air and the compressibility of air and water, as given by Brekhovskikh et al. (1973, eqs. 11 and 12. See also Supporting information). Namely the surface elevation is given by Hasselmann (1962),

$$\zeta_1(\mathbf{x}, t) = \sum_{\mathbf{k},s} Z^s_{1,\mathbf{k}} \exp\left[\mathrm{i}\left(\mathbf{k}\cdot\mathbf{x} - s\sigma t\right)\right], \tag{8}$$

where $Z^s_{1,\mathbf{k}}$ is the amplitude of the first order sea surface elevation for wavenumber $\mathbf{k}$ and propagation direction s and $s = \pm 1$ is a sign index that gives the direction of propagation relative the direction of the wave vector $\mathbf{k}$. The velocity potential in the water is given by,

$$\phi_w(\mathbf{x}, z, t) = \sum_{\mathbf{k},s} \Phi^s_{1,\mathbf{k}} \frac{\cosh(kz + kh)}{\cosh(kh)} \exp\left[\mathrm{i}\left(\mathbf{k}\cdot\mathbf{x} - s\sigma t\right)\right] \tag{9}$$

with

$$\Phi^s_{1,\mathbf{k}} = \frac{g}{\mathrm{i}\sigma} Z^s_{1,\mathbf{k}}. \tag{10}$$

In the air, the effects of gravity and compressibility (i.e. the right hand side terms in eq. 1), are less negligible, and we have,

$$\phi_a(\mathbf{x}, z, t) = \sum_{\mathbf{k},s} \frac{k}{k_a} \Phi^s_{1,\mathbf{k}} \exp\left[-k_a z + \mathrm{i}\left(\mathbf{k}\cdot\mathbf{x} - s\sigma t\right)\right] \tag{11}$$

with eq. 12 in Brekhovskikh et al. (1973),

$$k_a = k\left(\sqrt{1-\delta_a^2+\delta_a^4/2} - \delta_a^2/2\right) \simeq k\left(1-\delta_a^2\right) \tag{12}$$

where $\delta_a = \sqrt{g/k}/\alpha_a$. We note that half of this correction to k_a comes from the $\delta_a^2/2$ that is due to gravity, and the other half comes from the air compressibility.

Finally, in the ε^2 system, the wave spectrum acts as a forcing, coming through either the particular solutions that satisfy the wave equation with the right hand side, or from the boundary conditions between the different layers. In other words the wave forcing $\mathbf{\Lambda} = (\Lambda_i)_{1\leq i\leq N}$ is a vector on the right hand side of a matrix equation

$$\mathbf{M\Phi} = \mathbf{\Lambda}. \tag{13}$$

The only differences between all the theories discussed here are in the approximations of the boundary conditions between ocean and atmosphere and ocean and solid Earth. Mathematically, different terms are neglected in the coefficients of the matrix $\mathbf{M}$ or in the forcing vector $\mathbf{\Lambda}$, as detailed below.

Further extensions to multiple layers in the atmosphere and solid Earth give rise to different horizontally propagating modes, which correspond to zeros of the determinant of $\mathbf{M}$, for which a growth rate of the energy can be computed as done for seismic Rayleigh waves by Hasselmann (1963). The size of the matrix $\mathbf{M}$ grows by two lines and columns for each extra fluid layer, for which the two unknowns are one upward and one downward propagating potential amplitudes. For a solid layer there are four unknowns due to the presence of both compression and shear motions (see Hasselmann, 1963, eq. 1.4). The important difference with Hasselmann (1963) is that Λ_i was non-zero only for the sea surface pressure continuity equation in Hasselmann's case, whereas in

our case we will consider forcing in both the pressure and velocity equations. We also note that for finite water depth there is also a forcing term in the boundary condition for the ocean bottom pressure coming into Λ_3 (Ardhuin & Herbers, 2013).

2.1 Existing solutions

2.1.1 Case of infinite water depth - Brekhovskikh et al. (1973)

Brekhovskikh et al. (1973) considered only two layers, air and water, that are half spaces. As a result, for each frequency Ω and wavenumber vector $\mathbf{K}$, there are only two unknowns, one amplitude A for the velocity potential of upgoing acoustic waves in the atmosphere, and one amplitude W for downgoing acoustic waves or evanescent modes in the ocean. The approximation $m = \rho_a/\rho_w \ll 1$ removes the feedback of the atmospheric pressure on the air pressure, so that the atmosphere is only driven by the continuity of vertical velocities at the interface.

The coupling of air and water layers at $z = 0$ by the continuity of pressure and velocity gives a 2 by 2 matrix $\mathbf{M}$, with one line for the continuity of vertical velocity $w = \partial\phi/\partial z$ and the other for the continuity of pressure p ,

$$M_{1,1}A + M_{1,2}W = \Lambda_1 \tag{14}$$

$$M_{2,1}A + M_{2,2}W = \Lambda_2 \tag{15}$$

Following Brekhovskikh et al. (1973), we introduce the small parameters

$$\delta_a^2 = g/(k\alpha_a^2) \tag{16}$$

$$m = \rho_a/\rho_w \tag{17}$$

$$n = \alpha_a/\alpha_w \tag{18}$$

and we note that $|K/k| < 2\delta_a$. We now keep only the lowest order terms in δ_a and m, giving the

following matrix coefficients and right hand side (see Supporting information for details),

$$M_{1,1} = \nu_+ = \mathrm{i}\frac{\Omega}{\alpha_a}\cos\theta_a + \frac{k}{2}\delta_a^2 \tag{19}$$

$$M_{1,2} = -\mu_- = 2k\delta_a l - \frac{\delta_a^2}{2}kn^2 \tag{20}$$

$$M_{2,1} = -m\Omega^2 - g\mathrm{i}\frac{\Omega}{\alpha_a}\cos\theta_a \tag{21}$$

$$M_{2,2} = \Omega^2 \tag{22}$$

$$\Lambda_1 = \mathrm{i}s\Omega k\delta_a^2\left(2 - 2\sin^2\theta_a(1 - \frac{1}{2}\cos^2(\varphi_2 - \varphi)) + n^2\right) \tag{23}$$

$$\Lambda_2 = \frac{\mathrm{i}s\Omega}{\rho_w}p^s_{\mathrm{surf}}(\mathbf{K},\Omega) + o(\delta_a^2) \tag{24}$$

where we have defined

$$l = (\sin^2\theta_a - n^2)^{1/2} = n\cos\theta_w \quad \text{if} \quad \theta_a < \theta_{a0}. \tag{25}$$

Following Hasselmann (1963), we define the amplitude of the equivalent surface pressure induced at second order by the wave motion. Assuming that $kh \gg 1$ we take the following definition,

$$p^s_{\mathrm{surf}}(\mathbf{K},\Omega) = -2\rho_w \sum_{\mathbf{k}+\mathbf{k}'=\mathbf{K},\sigma+\sigma'=\Omega} \sigma\sigma' Z^s_{1,\mathbf{k}} Z^s_{1,\mathbf{k}'}. \tag{26}$$

In the following we will write p^s_{surf} instead of $p^s_{\mathrm{surf}}(\mathbf{K},\Omega)$.

The solution of the matrix equations eq. (14)–(15) is given by Cramer's rule,

$$A = \frac{\Lambda_1 M_{2,2} - \Lambda_2 M_{1,2}}{\det(\mathbf{M})}, \qquad \text{and} \qquad W = \frac{\Lambda_2 M_{1,1} - \Lambda_1 M_{2,1}}{\det(\mathbf{M})}. \tag{27}$$

Following details in Supporting material section S4.1, We find the amplitudes of the velocity potentials at the air-sea interface to be, for the water and air respectively,

$$W \simeq \frac{\mathrm{i}}{\rho_w}\frac{1}{2\sigma'}p^s_{\mathrm{surf}} \tag{28}$$

$$A \simeq \frac{R_a}{\rho_w}\frac{1}{2\sigma'}p^s_{\mathrm{surf}} \tag{29}$$

with

$$R_a = \frac{l - 2\delta_a\left[1 - \sin^2\theta_a\left(1 - \frac{1}{2}\cos^2(\varphi_2 - \varphi)\right) + \frac{5}{8}n^2\right]}{\cos\theta_a\,(1 - \delta_a l/2) - \mathrm{i}\,(\delta_a/4 + ml)}. \tag{30}$$

This form of R_a is identical to Brekhovskikh et al. (1973, eq. 22), except for the addition of one extra term $\cos\theta_a l\delta_a/2$ in the denominator, and a change in the sign of the denominator

term ml. As shown in Fig. 3, these two terms have a negligible impact on the solution, except for $\theta_a > 89.5°$, with less than 1% change in the total radiated acoustic power.

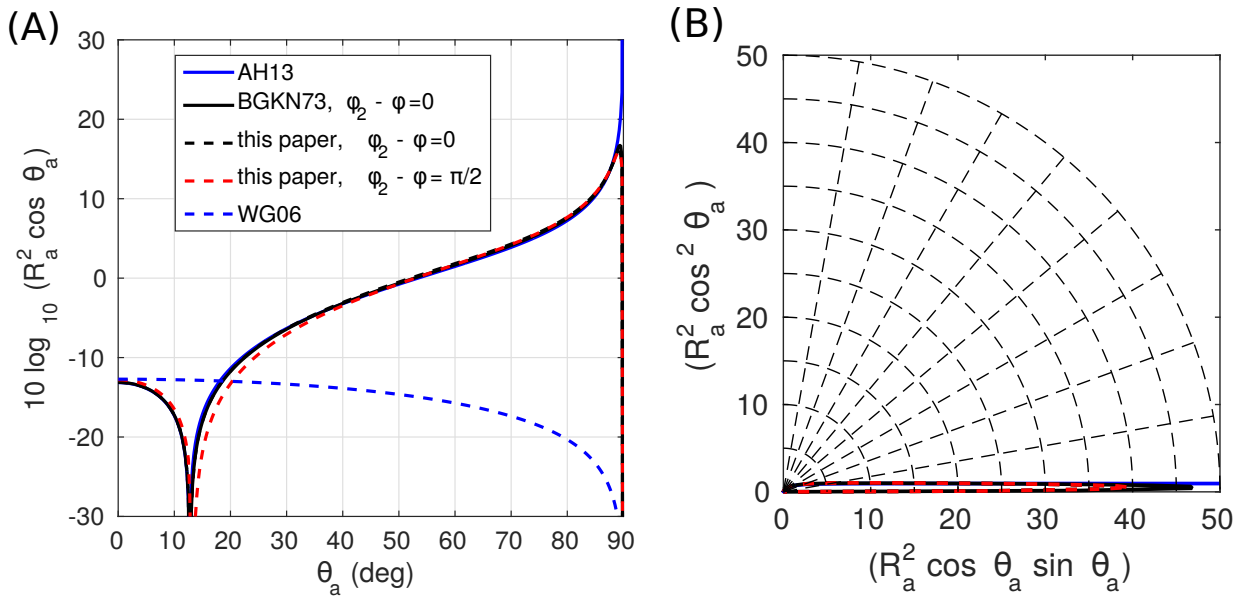

Figure 3. Patterns of acoustic pressure variance as a function of the elevation angle θ_a for an ocean wave period of 10 s, given by the different theories without ocean bottom, in cartesian (A), and polar (B) representation. Note that when the radiated power is considered, these patterns must be multiplied by $\sin\theta_a$ before integration over θ_a, as given by eq. (52). In general, as given by eq. (30) the radiated power is also a function of the relative azimuth of the first ocean wave train φ and the azimuth of the radiated acoustic power φ_2.

2.1.2 A simplified case - Ardhuin & Herbers (2013)

The solution given by Ardhuin et al. (2013) corresponds to the simplified solution given by eq. (21) in Brekhovskikh et al. (1973), with m and δ_a terms neglected, corresponding to an absence of feedback from the atmospheric pressure on the oceanic pressure, i.e. $M_{1,1} = 0$, and neglecting the right hand side of the acoustic wave equation in the air, i.e. $\Lambda_1 = 0$, giving

$$R_a = \frac{l}{\cos\theta_a} = \frac{\mathrm{i}(n^2 - \sin^2\theta_a)^{1/2}}{\cos\theta_a} \tag{31}$$

where we recall that l is imaginary for $\theta_a < \theta_{a0}$.

This simplified solution corresponds to infinite water depth. It presents a singularity for hori-

zontal acoustic propagation as $\cos\theta_a$ goes to zero. That singularity is removed when the feedback of the air on the water motion is taken into account.

2.1.3 Theory by Waxler and Gilbert (2006)

Following Brekhovskikh et al. (1973), Waxler & Gilbert (2006) showed that microbarom signals are due both to ocean radiation and to compression of the air by the surface motion, but Waxler & Gilbert (2006) neglected the effect of gravity in the air. As detailed in the Supporting information, accounting for gravity in the air changes their term $3\delta_a^2/2$ in their eq. (57) to $2\delta_a$ in eq. (32). we also note a change of sign from -2 to 1.5,

$$R_a^{\mathrm{WG06}} = \mathrm{i}n + 1.5\delta_a. \tag{32}$$

The particularity of the derivation by Waxler & Gilbert (2006) is the fact that they neglect the phase shift in the Green's function within the source region. They justified that approximation by assuming that the coherence length scale in the acoustic source is small compared to the acoustic wavelength. Here we do not use such an approximation, as detailed in the Appendix A, as the correlation function of the source is given by the pressure spectrum $p^s_{\mathrm{surf}}(\mathbf{K},\Omega)$ (our eq. 26) that overlaps with the acoustic wavelengths. The assumption in Waxler & Gilbert (2006) comes between their equations (50) and (51) and simplifies the expression of the radiation pattern in the atmosphere to a monopolar radiation pattern. It also reduces all expressions to their values for $\mathbf{K} = 0$, corresponding to strictly opposing wave trains, so that the evanescent ocean motions that correspond to $\theta_a > \theta_{a0}$ are not properly represented. Without this assumption, (Brekhovskikh et al., 1973) found that the radiation pattern is very different from a monopole, with an overwhelming radiation at very grazing angles, as illustrated in Fig. 1.A.

2.2 Generalization of Brekhovskikh et al. (1973) to a finite ocean depth

The first discussion of water depth effects on microbarom sources is due to Waxler et al. (2007). That work extended the analysis by Waxler & Gilbert (2006), limiting the water depth to h and

including an interface with a solid half space below. The velocity potential in the water is now

$$\phi_{w,2} = \sum \left(W_+ \mathrm{e}^{\mu_+ z} + W_- \mathrm{e}^{\mu_- z} \right) \mathrm{e}^{\mathrm{i}\Theta}. \tag{33}$$

with the complex wavenumber $\mu_\pm = g/(2\alpha_w) \pm \sqrt{K^2 - \Omega^2/\alpha_w^2} \simeq \pm\mu = \pm\sqrt{K^2 - \Omega^2/\alpha_w^2}$.

Taking an acoustic reflection coefficient $r = \rho_w \alpha_w / (\rho_s \alpha_s)$, Waxler et al. (2007) found the reflection condition for the down-going acoustic waves, with potential ϕ_w^- at the ocean bottom

$$W^+ = \frac{1+r}{1-r} \mathrm{e}^{2\mu h} W^-. \tag{34}$$

This gives,

$$R_a^{\mathrm{W07}} \simeq \mathrm{i}n \frac{r\cos(\Omega h/\alpha_w) + \mathrm{i}\sin(\Omega h/\alpha_w)}{\cos(\Omega h/\alpha_w) + \mathrm{i}r\sin(\Omega h/\alpha_w)} + 1.5\delta_a. \tag{35}$$

In order to properly consider the effect of the propagation angles, we can go back to the derivation of Brekhovskikh et al. (1973), now including an upgoing acoustic wave in the water layer. For oblique incidence we have to consider the contribution of compression waves and shear waves in the crust with velocities α_s and β. Defining the vertical wavenumbers in the the crust

$$\chi_p = \sqrt{K^2 - \frac{\Omega^2}{\alpha_s^2}}, \quad \text{and} \quad \chi_s = \sqrt{K^2 - \frac{\Omega^2}{\beta^2}}. \tag{36}$$

The reflection at the bottom generalizes to

$$r \simeq \frac{\Omega^4 \rho_w \chi_p}{\rho_s \mu \left[\left(\Omega^2 - 2K^2\beta^2\right)^2 - 4\beta^4 K^2 \chi_p \chi_s \right]}. \tag{37}$$

This is obtained by eliminating the potentials of the compression and shear motions in the crust, using the continuity of velocity and a zero tangential stress (see also Ardhuin & Herbers, 2013; Gualtieri et al., 2014).

When only the dominant terms are kept we find,

$$R_a = \frac{l}{\cos\theta_a} \frac{R}{Q} \tag{38}$$

with

$$R = \sinh(\mu h) + r\cosh(\mu h), \tag{39}$$

$$Q = \cosh(\mu h) + r\sinh(\mu h). \tag{40}$$

In the case $\theta_a = 0$, eq. (38) corresponds to the first term of eq. (35).

When going to first order in δ_a and m, the problem can be simplified by neglecting the effect of gravity in the water layer, which contributed to the n^2 term in the numerator of eq. (30). This gives $-\mu_- = \mu_+ = \mu$. It is then more simple to eliminate the amplitude W^- by using the bottom boundary condition on the vertical velocity. This amounts to replacing $-\mu_-$ by $-2\mu R\mathrm{e}^{-\mu h}/(1+r)$ in $M_{1,2}$ and Ω^2 by $2Q\Omega^2\mathrm{e}^{-\mu h}/(1\ +\ r)$ in $M_{2,2}$, giving,

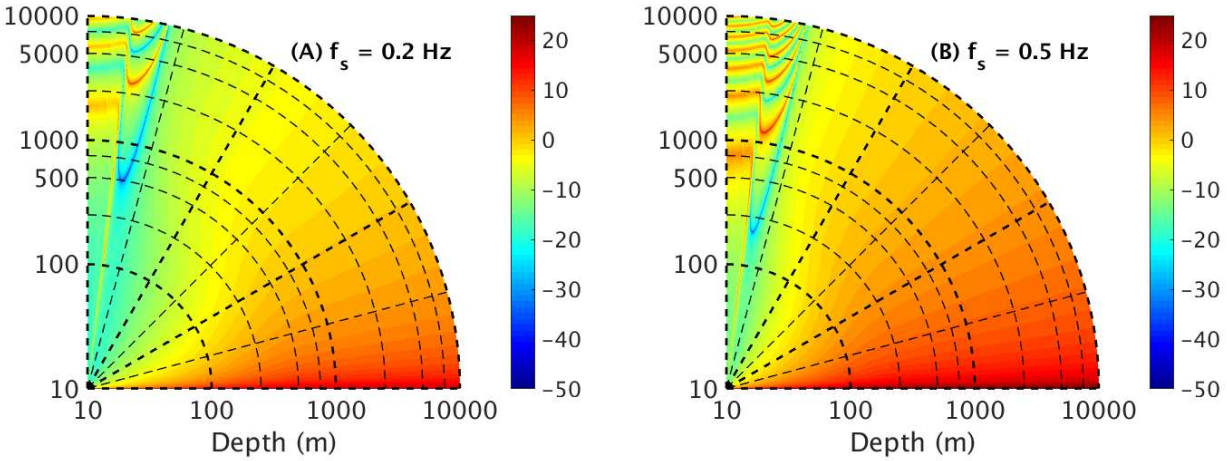

Figure 4. Radiation patterns of $10\log_{10}|R_a|$ according to eq. (41) for (A) $f_s = 0.2$ Hz , (B) $f_s = 0.5$ Hz with $f_s = \Omega/2\pi$ - polar representation against the angle θ_a and the depth h.

$$R_a = \frac{lR - 2\delta_a Q\left[1 - \sin^2\theta_a\left(1 - \frac{1}{2}\cos^2(\varphi_2 - \varphi)\right)\right]}{\cos\theta_a\left(Q + R\delta_a l/2\right) - \mathrm{i}\left(Q\delta_a/4 + Rml\right)} \tag{41}$$

Table 2. Summary of differences between models, with R_a defined on eq. (29)

Model	depends on θ_a	depth	compressible	gravity	R_a
BGKN73	✓	∞	✓	✓	eq. (30)
AH13	✓	∞	×	×	eq. (31)
WG06	×	∞	✓	×	eq. (32)
W07	×	any	✓	×	eq. (35)
this paper	✓	any	✓	✓	eq. (41)

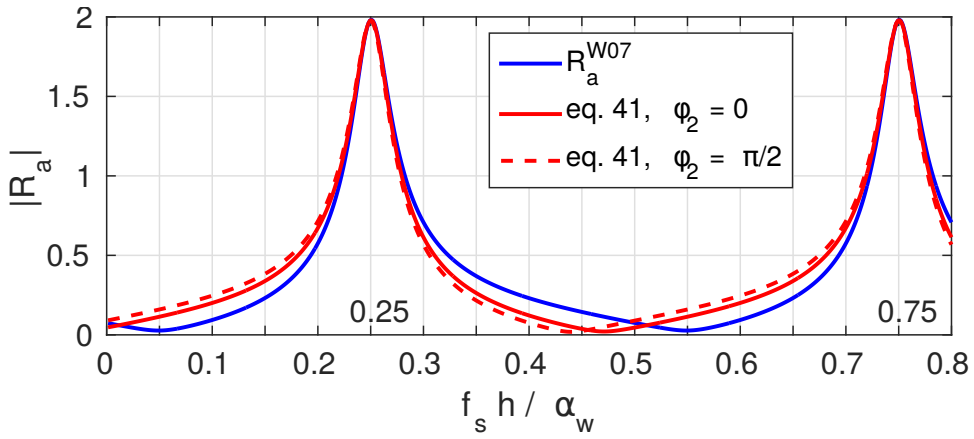

Figure 5. Magnitude of the velocity potential amplification from the water to the air, R_a, as a function of the ratio of the water depth and acoustic wavelength, in the case of vertical propagation, i. e. $\theta_a = 0$. For $f_s = 0.2$ Hz, the two peaks corresponds to depths of 1900 and 5600 m. Here we have used $\alpha_s = 5540$ m/s, $\beta = \alpha_s/\sqrt{3}$, $\rho_s = 2500$km/m^3.

2.3 Radiated acoustic power as a function of elevation and azimuth

We introduce the spectral density of the homogeneous (propagating) pressure field at $z = 0$, in the three spectral dimensions (K_x, K_y, f_s) using the Fourier amplitude of $p_{a,2}$ at $z = 0$, obtained from the average over realizations of the sea state, represented by angular brackets, of the pressure amplitude squared,

$$F_{p,2h}(\mathbf{K}, f_s) = 2 \lim_{\Delta K_x \to 0, \Delta K_y \to 0, df_s \to 0} \frac{\left\langle \left| P^+_{2,h} \right|^2 (\mathbf{K}, f_s) \right\rangle}{\Delta K_x \Delta K_x \Delta f_s} \tag{42}$$

Given the dispersion relation of ocean surface gravity waves in deep water, the Jacobian of the transformation from (k_x, k_y) to (f, φ) is $2\pi k/(\partial\sigma/\partial k) = 4\pi\sigma^3/g^2$.

We now define the ocean wave spectrum as

$$\begin{aligned} E(f,\varphi) &= \frac{4\pi\sigma^3}{g^2} E(k_x, k_y) = 2 \lim_{\Delta k_x \to 0, \Delta k_y \to 0} \frac{|Z^+_{\mathbf{k}}|^2}{\Delta K_x \Delta K_y} \frac{4\pi\sigma^3}{g^2} \\ &= 2 \lim_{\Delta f \to 0, \Delta\varphi \to 0} \frac{|Z^+_{\mathbf{k}}|^2}{\Delta f \Delta\varphi}. \end{aligned} \tag{43}$$

We use eq. (26) and replace the amplitude $P^+_{2,h}$ by $\mathrm{i}(\sigma + \sigma')\rho_a A$, namely,

$$P^+_{2,h} = \frac{\mathrm{i}\rho_a(\sigma + \sigma')}{\rho_w 2\sigma'} R_a p^+_{\mathrm{surf}}. \tag{44}$$

This gives,

$$2\left|P^{+}_{2,h}\right|^2 = 2\rho_a^2\left|R_a\right|^2\sigma^2(\sigma+\sigma')^2\left|\sum_{\mathbf{k}+\mathbf{k}'=\mathbf{K},\sigma+\sigma'=\Omega} Z_{1,\mathbf{k}}Z_{1,\mathbf{k}'}\right|^2 \tag{45}$$

$$= \sigma^2(\sigma+\sigma')^2\rho_a^2\left|R_a\right|^2 \sum_{\mathbf{k}+\mathbf{k}'=\mathbf{K},\sigma+\sigma'=\Omega} 2\left|Z^{+}_{1,\mathbf{k}}\right|^2 2\left|Z^{+}_{1,\mathbf{k}'}\right|^2, \tag{46}$$

where the last equality is obtained by considering that each pair of wavenumbers $(\mathbf{k}_1, \mathbf{k}_2)$ is counted twice, a first time when $\mathbf{k} = \mathbf{k}_1$ and $\mathbf{k}' = \mathbf{k}_2$ and a second time when $\mathbf{k} = \mathbf{k}_2$ and $\mathbf{k}' = \mathbf{k}_1$. This is well understood when considering the simplest form with the ocean wave field consisting of only two cosine waves (See Supporting information, eqs. S124–S128).

Taking the limit to continuous sums and using a change of variable from (k_x, k_y, k'_x, k'_y) to (f_s, φ, K_x, K_y), with $K_x = k_x + k'_x$, $K_y = k_y + k'_y$ and $f_s = (\sqrt{gk} + \sqrt{gk'})/(2\pi)$ the Jacobian of the coordinate transform is

$$\det\left(\frac{\partial f_s \partial\varphi \partial K_x \partial K_y}{\partial k_x \partial k_y \partial k'_x \partial k'_y}\right) = \begin{vmatrix} g\cos\varphi/(4\pi\sigma) & -\sin\varphi/k & 1 & 0 \\ g\sin\varphi/(4\pi\sigma) & \cos\varphi/k & 0 & 1 \\ g\cos\varphi'/(4\pi\sigma') & 0 & 1 & 0 \\ g\sin\varphi'/(4\pi\sigma') & 0 & 0 & 1 \end{vmatrix}$$

$$= \frac{g^2}{4\pi\sigma^3\sigma'}\left[\sigma' - \sigma\cos\left(\varphi-\varphi'\right)\right], \tag{47}$$

and gives

$$\int F_{p,2h}(\mathbf{K}, f_s)\mathrm{d}K_x\mathrm{d}K_y\mathrm{d}f_s = \rho_a^2\int \sigma^2(\sigma+\sigma')^2\left|R_a\right|^2 E(k_x,k_y)E(k_x,k_y)\mathrm{d}k_x\mathrm{d}k_y\mathrm{d}k'_x\mathrm{d}k'_y$$

$$= \rho_a^2\int \sigma^2(\sigma+\sigma')^2\left|R_a\right|^2 \frac{E(k_x,k_y)E(k'_x,k'_y)4\pi\sigma^3\sigma'}{g^2\left[\sigma' - \sigma\cos\left(\varphi-\varphi'\right)\right]}\mathrm{d}f_s\mathrm{d}\varphi\mathrm{d}K_x\mathrm{d}K_y.$$

Now we use the unicity of the Fourier transform to identify the spectral density in the left and right hand sides, and using eq. (43) gives

$$F_{p,2h}(\mathbf{K}, f_s) = \frac{1}{2}\rho_a^2 g^2 f_s \int_0^{2\pi} \frac{\sigma^2(\sigma+\sigma')}{\sigma'^2}\left|R_a\right|^2 \frac{E(f,\varphi)E(f',\varphi')}{\sigma' - \sigma\cos\left(\varphi-\varphi'\right)}\mathrm{d}\varphi. \tag{48}$$

We note that the form of the acoustic power given by eq. (48) is generally a function of the direction φ_2 of the horizontal wave vector $\mathbf{K}$ of the acoustic waves.

In the limit $\delta_a \ll 1$, this simplifies to a horizontally isotropic form

$$F_{p,2h}(\mathbf{K}, f_s) \simeq \frac{1}{2}\rho_a^2 g^2 f_s \left|R_a\right|^2 \int_0^{2\pi} E(f,\varphi)E(f,\varphi+\pi)\mathrm{d}\varphi. \tag{49}$$

This last expression, with $|R_a|^2 \simeq |(\sin^2\theta_a - n^2)|/\cos^2\theta_a$, is the one used by Ardhuin & Herbers (2013).

The pressure spectrum can be re-written as a directional spectrum, with the proper change of coordinate this gives,

$$F_{p,2h}(\theta_a, \varphi_2, f_s) = \frac{4\pi^2 f_s^2 \cos\theta_a \sin\theta_a}{\alpha_a^2} F_{p,2h}(\mathbf{K}, f_s). \quad (50)$$

When δ_a terms are kept with eq. (48), the acoustic power radiated by the ocean surface in direction φ_2 can be integrated in any range of incidence angles $\theta_{a,1}$ to $\theta_{a,2}$,

$$P(\theta_{a,1}, \theta_{a,2}, f_s, \varphi_2) = \frac{2\pi^2 \rho_a g^2}{\alpha_a^3} f_s^3 \int_{\theta_{a,1}}^{\theta_{a,2}} \sin\theta_a \cos\theta_a \times \int_0^{2\pi} \frac{\sigma^2(\sigma+\sigma')\,|R_a|^2\, E(f,\varphi)E(f,\varphi')}{\sigma'^2\left[\sigma' - \sigma\cos\left(\varphi-\varphi'\right)\right]} \mathrm{d}\varphi \mathrm{d}\theta_a, \quad (51)$$

Taking the isotropic form (49) the radiated acoustic power becomes isotropic and the sum over all directions is 2π times eq. (51), giving

$$2\pi P(\theta_{a,1}, \theta_{a,2}, f_s, \varphi_2) = \frac{4\pi^3 \rho_a g^2}{\alpha_a^3} f_s^3 H(f_s/2) \int_{\theta_{a,1}}^{\theta_{a,2}} \sin\theta_a \cos\theta_a\, |R_a|^2\, \mathrm{d}\theta_a, \quad (52)$$

with units of W/m^2/Hz, where the so-called 'Hasselmann integral' can be defined from the 'overlap integral' (Farrell & Munk, 2008) and the wave spectrum in frequency,

$$H(f) = [E(f)]^2\, I(f) = \int_0^{2\pi} E(f,\varphi)E(f,\varphi+\pi)\mathrm{d}\varphi. \quad (53)$$

The total integrated radiated power, with units of W/m^2, is obtained by integrating eq. (52) across acoustic frequencies f_s. In Fig. 6, the mean acoustic intensity over the year 2018 is represented for six ranges of vertical incidence angles. The distribution pattern of sources for the vertical angles $[0°, 5°]$ shows the effect of bathymetry, unlike the near-horizontal angles with similar patterns depending almost solely on the Hasselman integral. For near-vertical angles - $[5°, 10°]$ and $[10°, 15°]$ - the distribution pattern is not continuous, there are resonant points all over the globe. The acoustic intensity is higher for near-horizontal angles, as predicted in Fig. 4.

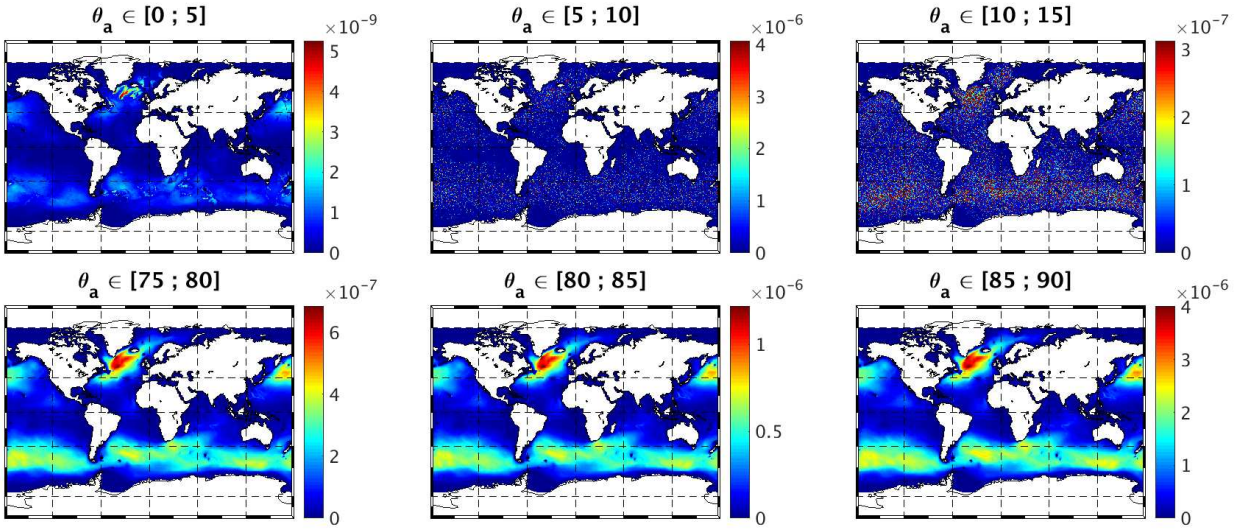

Figure 6. Acoustic intensity in W/m^2 - computed by integrating eq. 52 over f_s - for 6 ranges of incidence angles : A) $[\theta_{a,1}, \theta_{a,2}] = [0°, 5°]$, B) $[\theta_{a,1}, \theta_{a,2}] = [5°, 10°]$, C) $[\theta_{a,1}, \theta_{a,2}] = [10°, 15°]$, D) $[\theta_{a,1}, \theta_{a,2}] = [75°, 80°]$, E) $[\theta_{a,1}, \theta_{a,2}] = [80°, 85°]$, F) $[\theta_{a,1}, \theta_{a,2}] = [85°, 90°]$. Mean of a 3-hourly model over 2018. These were computed from numerical ocean wave model output already described by Rascle & Ardhuin (2013) and available at (ftp://ftp.ifremer.fr/ifremer/ww3/), using the WAVEWATCH III® code (The WAVEWATCH III ® Development Group, 2016)

.

3 PRACTICAL IMPLICATIONS AND DISCUSSION

3.1 Near-vertical propagation and Rayleigh wave overestimation

We note that for vertical propagation ($\theta_a = 0$) the effect of the finite depth changes the amplitude by a factor that ranges from 0.125 to 8.5 with sharp maxima corresponding to the organ pipe resonance at $h = (0.25 + n/2)\alpha_w/f_s$, as illustrated in Fig. 5, which is similar to fig. 11 in Ardhuin & Herbers (2013).

The behaviour at other angles is very interesting as θ_a goes through the different regimes of associated seismic waves, from P-waves for $\sin\theta_a < \alpha_a/\alpha_s$ – i.e. $\theta_a < 3.41°$ for our choice of parameters – to Rayleigh waves, which usually contain most of the microseism signal, with $\arcsin \alpha_a/\beta < \theta_a < \arcsin \alpha_a/\alpha_w$ corresponding to a range of 5.9 to 12.7° which is shaded in Fig. 7.

The two maxima that appear in the Rayleigh domain in Fig. 7.A are the two modes that can exist at 5000 m depth, whereas only one mode can exist at 1900 m depth. As discussed by Ard-

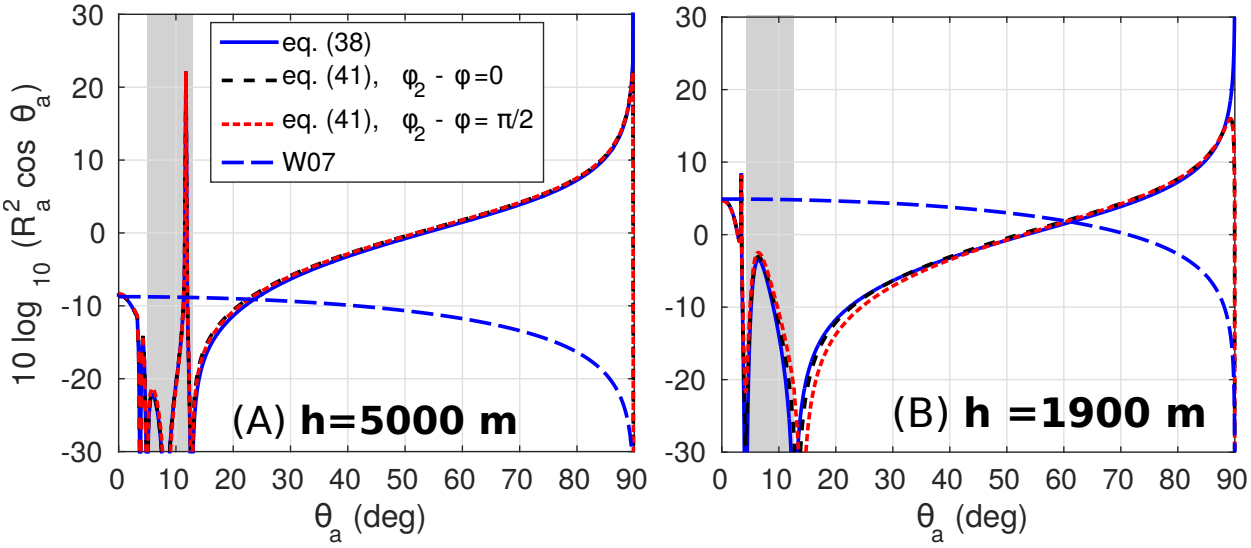

Figure 7. Radiation patterns for an ocean wave period of 10 s, given by the different theories with an ocean bottom at (A) $h = 5000$ m, (B) $h = 1900$ m. Note that when the radiated power is considered, these patterns must be multiplied by $\sin\theta_a$ before integration over θ_a, as given by eq. 52. The shaded region corresponds to the domain of seismic Rayleigh waves with $\arcsin(\alpha_a/\beta) < \theta_a < \arcsin(\alpha_a/\alpha_w)$.

huin & Herbers (2013) the depth and frequency at which the amplification is maximum is shifted compared to Fig. 5. This is because the acoustic water component of these Rayleigh modes do not propagate vertically but obliquely at an angle θ_w, as shown in Fig. 1.B, giving a resonance at $h = (0.25 + n/2)\alpha_w/(f_s \cos\theta_w)$.

Our model certainly overestimates the amplitude of these Rayleigh waves and associated microbaroms because we looked for solutions that are homogeneous in space and time. In the solution given above, the leak of energy to the atmosphere is the only loss of energy of the Rayleigh waves and it compensates the source of energy from the local waves. In reality, two important effects limit the microbarom amplitude to a much lower level. First, the ocean storm area of microbarom generation may not be large enough to reach the stationary solution, and second there is a much larger (6 to 1000 times or more) sink of seismic energy, due to the presence of fluid in the crust, varying with the age of the crust (Stutzmann et al., 2012). The dissipation rate of the energy E is generally parameterized as proportional to $dE/dt = -\Omega E/Q_R$ where Q_R is of the order of 200 to 1000. Including this effect in the present paper amounts to replacing Ω by $\Omega(1 - \mathrm{i}/(2Q_R))$ which is done in Fig. 8. In other words, the Rayleigh wave energy is overestimated when dissi-

pation in the crust is neglected because in that case, the leakage of Rayleigh wave energy to the atmosphere is the loss of seismic energy. Hence, our calculation has a seismic attenuation with a very large quality factor $Q_{\max} = \Omega E/S$, where S is the source of seismic energy that equals the radiated power given by eq. (52): $P(\arcsin(\alpha_a/\beta), \arcsin(\alpha_a/\alpha_w), f_s)$. Taking twice the kinetic energy in the water column as a lower bound for the total energy we find that, for $h = 5000$ m and $f_s = 0.2$ Hz, $Q_{\max} > 10^6$ (Supporting information, section S6.3), meaning that the present solution overestimates the real microbarom amplitude by a factor that exceeds $Q_{\max}/Q_R > 1000$.

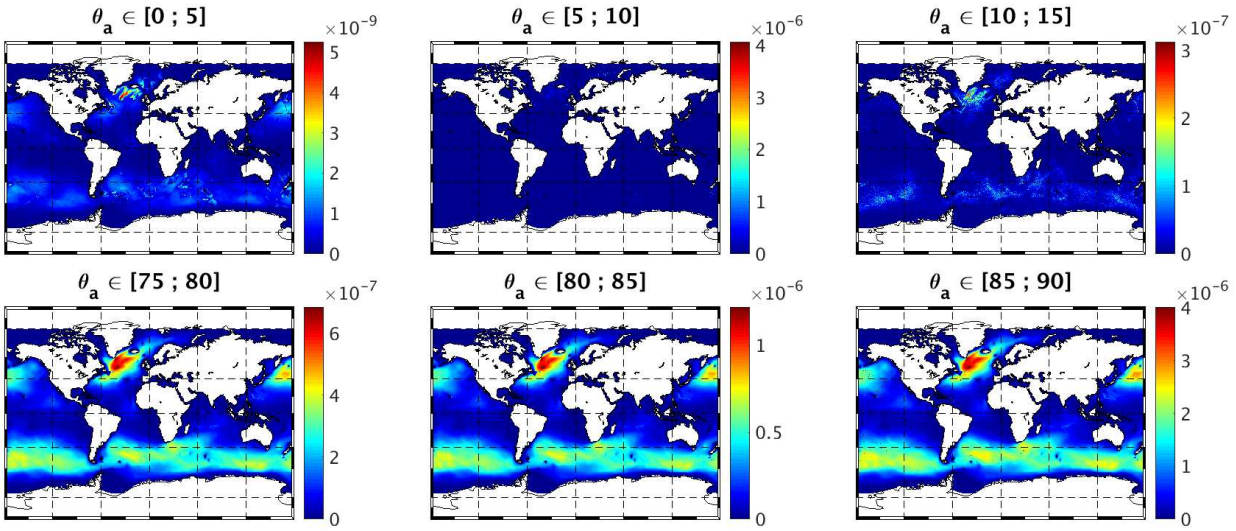

Figure 8. Same as Fig. 6 replacing Ω by $\Omega(1 - \mathrm{i}/(2Q_R)$ with $Q_R = 200$ in order not to overestimate Rayleigh wave energy.

Alternatively, instead of looking for the homogeneous solution to the atmosphere-ocean-crust problem, we can use solutions for the ocean-crust problem with an energy that grows over the source region (Hasselmann, 1963; Ardhuin & Herbers, 2013), and compute the microbaroms radiated by microseisms (free Rayleigh waves). These microbaroms are radiated both in the source region of microseism but also all along the propagation path of the Rayleigh waves, even on land. For example, a huge microseism with amplitude $a = 10$ micrometers vertical displacement of the sea or land surface corresponds to an energy flux $\rho_a \alpha_a \Omega^2 a^2/2$ of only 3×10^{-8}W/m^2 for $f_s = 0.2$ Hz. This is 2000 times smaller than the peak power measured by Bowman & Lees (2018). It is thus unlikely that these measurements are dominated by near-vertical propagating sound waves. Indeed, the near-horizontal energy level is usually much stronger.

3.2 Radiation patterns as a function of azimuth

The variation of the radiated acoustic power with azimuth φ_2 has not been described before as most studies focused on near-vertical radiation ($K = 0$). In eq. (51) there are two reasons why the radiated power varies with φ_2 .

As expressed by the general form given in eq. (51), the radiated power varies with azimuth $\varphi 2$ due to the general form of R_a, as shown in figures 3 and 5 but that variation is limited to a few percent. More important is the fact that the Hasselmann integral $H(f)$ is modified by the interaction of $E(f, \varphi)$ with $E(f', \varphi')$ instead of $E(f, \varphi + \pi)$, and should be replaced by,

$$H(f, \varphi_2) = \int_0^{2\pi} \frac{\sigma^2(\sigma + \sigma')E(f, \varphi)E(f, \varphi')}{\sigma'^2 \left[\sigma' - \sigma \cos\left(\varphi - \varphi'\right)\right]} \mathrm{d}\varphi. \tag{54}$$

.

Following the classification in (Ardhuin et al., 2011), the oceanic conditions in which the Hasselmann integral takes the largest values correspond to 'class III' events, with two narrow swells propagating in opposite directions. These are also conditions in which $E(f', \varphi')$ may be most different from $E(f, \varphi + \pi)$.

3.2.1 Case of analytical ocean wave spectra

To illustrate this effect, we take an example of a family of wave spectra adapted from the case discussed in (Obrebski et al., 2012). This family of spectra is defined by the analytic expression,

$$E(f, \varphi) = E_0 \left[\mathrm{e}^{-\frac{(f-f_1)^2}{2f_2^2} - \frac{(\varphi-\varphi_1)^2}{2\varphi_3^2}} + \mathrm{e}^{-\frac{(f-f_3)^2}{2f_4^2} - \frac{(\varphi-\varphi_4)^2}{2\varphi_5^2}} \right], \tag{55}$$

where the f_1, f_2, f_3, f_4 parameters define the peak frequency and width for the two swell trains, and φ_1, φ_3, φ_4, φ_5 define the mean direction and width. The present theory is not restricted to this family of spectra and generally applies to any wave spectrum. Such an analytical form is particularly useful for testing the influence of the discretization when the spectrum is given by a numerical model.

Fig. 9.A shows this spectrum transformed to wavenumber space $E(k_x, k_y) = g^2 E(f, \varphi)/4\pi\sigma^3$, with the mean frequency and direction set to $f_1 = 0.066$ Hz, $f_3 = 0.066$ Hz, $\varphi_1 = 90°$, $\varphi_3 = 270°$,

the widths $f_2 = 0.007$ Hz, $f_2 = 0.007$ Hz, $\varphi_4 = 8°$, $\varphi_5 = 8°$, and the normalization factor $E_0 = 20\text{m}^2/\text{Hz}$, giving a significant wave height of 2 m.

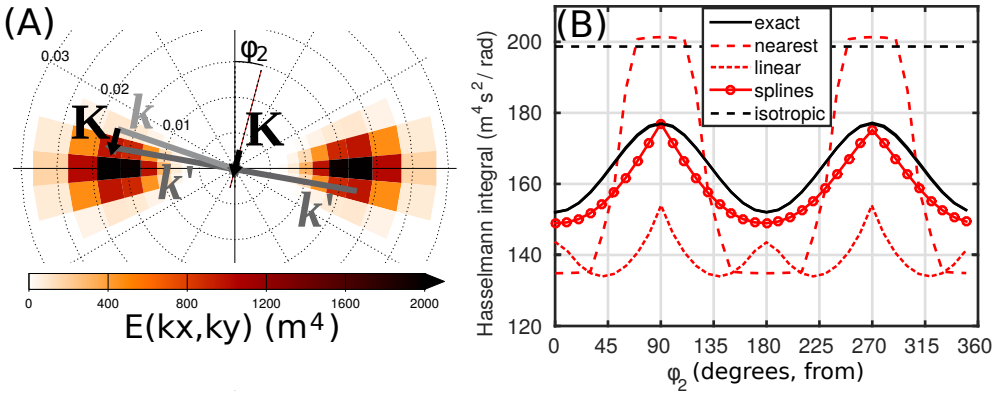

Figure 9. (A) Example spectrum discretized with 36 directions and frequency exponentially spaced with an 1.1 increment from one frequency to the next, typically used in numerical wave models. The spectral density of the ocean waves is shown in colors, in directions from where the waves come. (B) Resulting integrals for the acoustic frequency $f_s = 0.13$ Hz, and horizontal propagation ($\theta_a = 90°$, $K = 0.0025$ rad/m). Three methods were used to compute the integral: the analytic spectral expression or interpolation of the discrete spectrum using nearest neighbor or linear interpolation.

The azimuthal variation of the generalized Hasselmann integral, as given by eq. (54) is illustrated in Fig. 9.B.

The exact calculation uses the analytic expression of the spectrum, and exhibits variations of 7% of the radiated acoustic power as a function of φ_2, with a maximum in the direction of the waves because the spectrum, in k-space is more narrow in the k_y than in the k_x direction and when K is aligned with the y-axis, as shown, the wavenumber vector $\mathbf{k}'$ falls away from the peak faster than when K is aligned with the x-axis. For the present example the azimuthal variation goes away when the directional spread is increased from 8 to 12° and it has a maximum at 0 and 180° for wider directional spectra.

The practical estimation of the integral is very sensitive to the discretization used, which is not an issue when K is much smaller than the discretization of the spectrum and the isotropic form can be used. Numerical wave models that typically use 10% increments from one frequency to the next and 24 or 36 directions do not resolve very well the narrow swell peaks such as those in

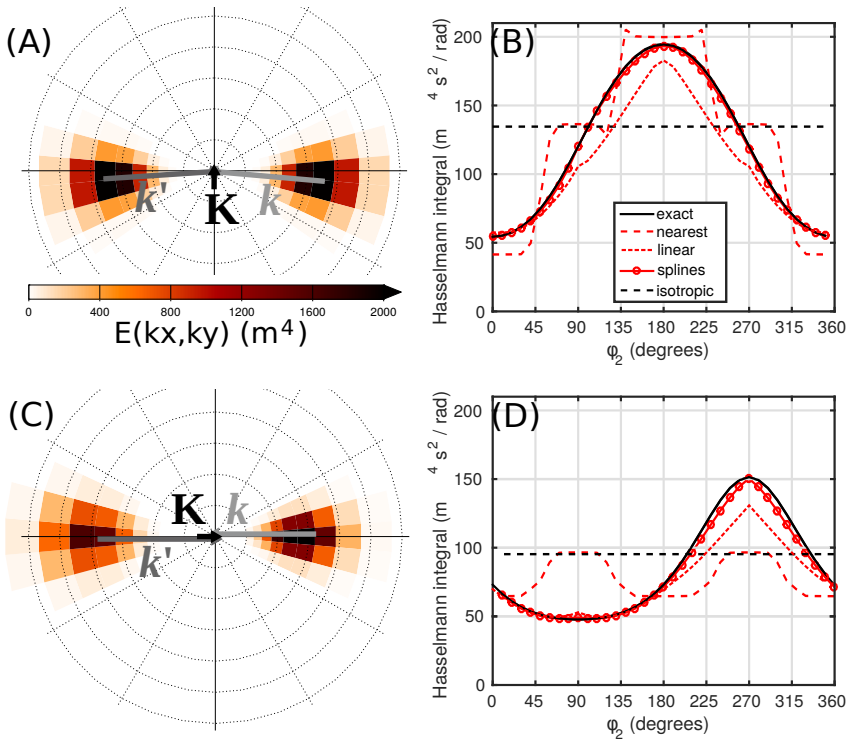

Figure 10. Same as Fig. 9 with different ocean wave spectra (A) that have mean directions shifted by 5 degrees to $\varphi_1 = 95°$ and $\varphi_3 = 265°$ producing the Hasselmann integral in (B). The wave spectrum in produces the Hasselmann integral in (D), with a peak frequencies shifted by 0.006 Hz to $f_1 = 0.072$ Hz and $f_2 = 0.060$ Hz. For both cases, the configuration of $\mathbf{k}$ and $\mathbf{k}'$ that gives the largest contribution to the Hasselman integral in indicated in (A) and (C) with arrows.

Fig. 9.A. As a result, a linear interpolation underestimates the integral because the peak appears narrower. On average this is corrected by using the nearest point, but that approach can exaggerate the anisotropy of the acoustic source.

Besides causing anisotropic sources when two swell peaks are exactly opposed, the generalized integral may broaden the region where sources are significant, as shown in Fig. 10, because it allows a wider range of directions and frequencies to interact compared to $\mathbf{k} = \mathbf{k}'$ in the simplified form.

3.2.2 General case using numerical wave model output

In order to test this idea, we have computed the Hasselmann integral from wave-model output which are 'real' spectrum (non idealised spectrum) with the usual form and its generalization in the case of the event discussed by Bowman & Lees (2018). Fig. 11 shows modeled maps of wave

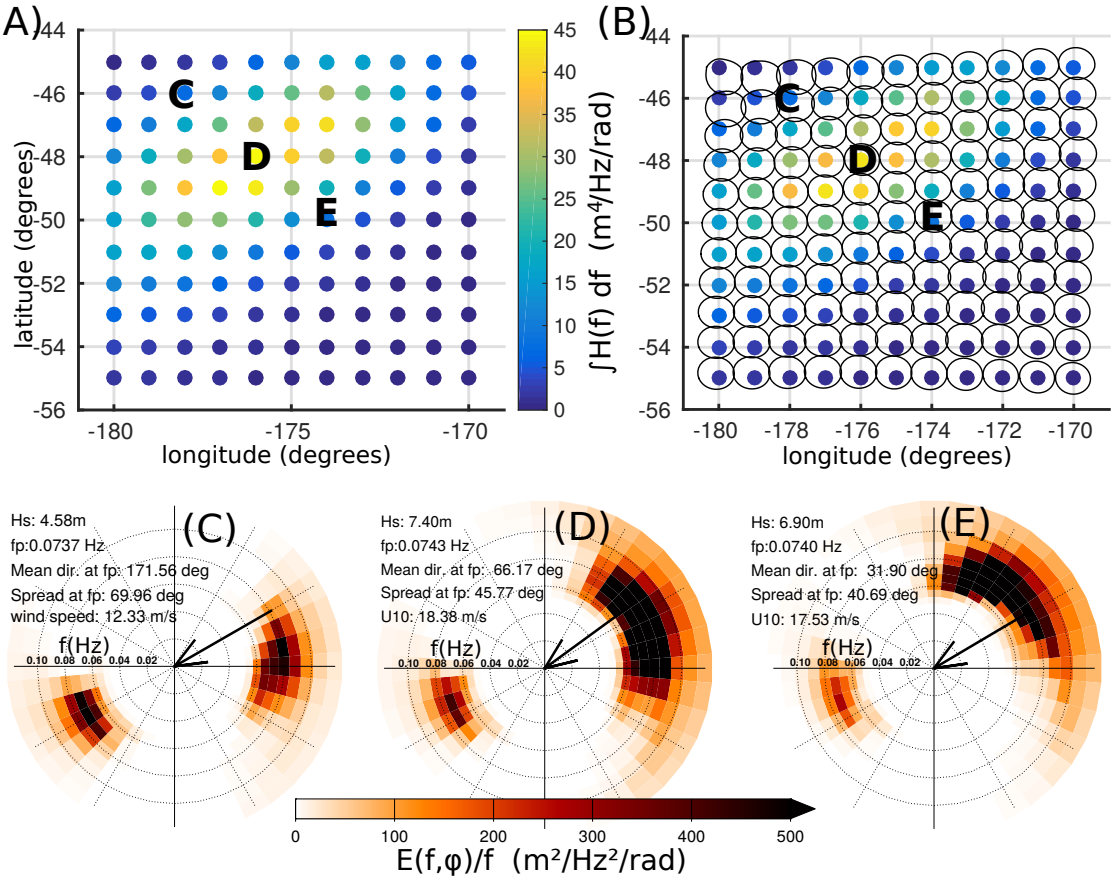

Figure 11. Maps of the Hasselmann Integral for (A) the isotropic and (B) non-isotropic expressions. In (B) the black curve around each location represents the Hasselmann integral estimated as a function of the acoustic propagation azimuth, and plotted in direction from where the acoustic waves are coming and normalized so that the average radius is half the distance between neighboring locations. (C), (D) and (E) are showing modeled directional spectra at the C , D, and E locations mentioned in (A) and (B). The large arrows indicate the wind direction, from the north-east, associated to a broad windsea spectrum which opposes a more narrow swell spectrum from the south-west.

source magnitude, in color, using the isotropic or azimuth-dependent form of the Hasselmann integral over a 10 degree by 10 degree region located to the south-east of New Zealand, valid for May 2016, at 06:00 UTC. The wave model used here is very similar to the one used in Ardhuin et al. (2015), with a number of discrete directions increased from 24 to 36. This strong microbarom source is associated to a strong local wind, up to 18 m/s, blowing against swell coming from a remote storm, typical of a class-III event described by Ardhuin et al. (2011).

The first striking result is that the colors are very similar, with a correlation of 0.9998, meaning that the simplified isotropic form is a good approximation of the total radiated power, at least for

this example. We also note that the highest sources are most isotropic, such as at location D in Fig. 11.B. Where sources are more strongly radiated in one direction, such as at locations C and E, this is due to a gradual shift in the direction of both interacting wave trains, the swell from the south-west has a local direction that is close to 240° at C, and 255° at E, and the time evolution of the local wind means that the wind sea is rather from the East at C and the North-East at E. In this particular example this gives a dominant radiation from the south-east at C and the north at E.

When averaged over the entire area, the difference between the radiated power in any given direction and the isotropic solution is less than 15%, suggesting that the isotropic approximation may be accurate enough for most applications.

4 CONCLUSIONS

In this paper we have reviewed and unified the microbarom source theories developed by Brekhovskikh et al. (1973) and Waxler et al. (2007). A prominent feature of Brekhovskikh et al. (1973), that was not taken into account by Waxler et al. (2007), is the radiation pattern as a function of the elevation angle θ_a. In Waxler et al. (2007), the radiation pattern is monopolar due to an assumed lack of coherence of the sources at scales comparable to the acoustic wavelength. In Brekhovskikh et al. (1973) the acoustic power at near-horizontal incidence that up to 1000 times larger because the main coupling of water and air via the vertical velocity of the air-sea interface gives a much stronger amplification for grazing angles. Including finite depth ocean effects in Brekhovskikh et al. (1973) model is only relevant for near-vertical propagation, and has almost no effect on the predicted dominant near-horizontal propagation of infrasound. For shallow propagation angles that generally correspond to ground-based measurements (i.e. $\theta_a > 40°$, relative to vertical) Brekhovskikh et al. (1973)'s formulation is compared to the more complete depth-dependent model presented here. We find that in regions of water depths under 1000 m, which cover 10% of the total ocean surface, - Brekhovskikh et al. (1973)'s formulation overestimates the source amplitude and underestimates it for deeper waters. On average there is a 7% understimation and Brekhovskikh et al. (1973) gives overall acceptable results, with a negligible effect of the water depth for near-horizontal propagation angles.

For near-vertical propagation, the generation of microbaroms involve both a source mechanism similar to the one of microseism dominated by the non-linear interaction of near-opposing waves, and Rayleigh waves propagating away from microseism sources. However, the associated acoustic power is at least 2 orders of magnitude lower than the near-horizontal radiated power. These vertical angles can be of interest for altitude measurements such as balloon measurements (Bowman & Lees, 2018); in such situation, the bathymetry can still impact the received signal. The horizontal anisotropy of the source has also been investigated, leading to the conclusion that, for computational applications, the isotropic approximation may be accurate enough and could then be used. Hence, the discretization of the wave spectrum might not be an issue.

Beyond theoretical issues, efforts should be pursued to validate the proposed model by considering available observations of infrasound ambient noise as recorded by the global infrasound network of the International Monitoring System (IMS) (Ceranna et al., 2019). For practical applications, further developments of a numerical model are needed to propagate microbarom signals over large distances through a realistic atmosphere. The implementation of this source model, based on a state-of-the-art numerical wave model (Ardhuin, 2019) should help building a global and time-dependent reference database. Exploiting this database of oceanic noise sources will be useful for developing middle-atmospheric remote sensing methods. The evaluation of infrasound ambient noise model is essential in the context of the future verification of the Comprehensive nuclear Test Ban Treaty (CTBT), as accurate atmospheric models are basic prerequisite to assess the IMS network performance in higher resolution, reduce source location errors, and improve source characterization methods.

ACKNOWLEDGMENTS

The ocean wave spectra from which the Hasselmann integral were computed with the WAVEWATCH III wave-action model, and these spectra are available at ftp://ftp.ifremer.fr/ifremer/ww3/.

The research leading to these results was partly performed during the course of the ARISE2 project (http://ARISE-project.eu) funded by the European Commission Horizon 2020 (grant agree-

549 ment 65398). This work was also supported by Agence Nationale de la Recherche under grant
550 ANR-14-CE01-0012 'MIMOSA'.

551 This paper owes much to discussion with Roger Waxler, his review and the review of one
552 anonymous reviewer.

References

Ardhuin, F., 2019. *Ocean waves in geosciences*.

Ardhuin, F. & Herbers, T. H. C., 2013. Noise generation in the solid earth, oceans and atmosphere, from nonlinear interacting surface gravity waves in finite depth, *J. Fluid Mech.*, **716**, 316–348.

Ardhuin, F., Stutzmann, E., Schimmel, M., & Mangeney, A., 2011. Ocean wave sources of seismic noise, *J. Geophys. Res.*, **116**, C09004.

Ardhuin, F., Lavanant, T., Obrebski, M., Marié, L., Royer, J.-Y., d'Eu, J.-F., Howe, B. M., Lukas, R., & Aucan, J., 2013. A numerical model for ocean ultra low frequency noise: wave-generated acoustic-gravity and Rayleigh modes, *J. Acoust. Soc. Amer.*, **134**(4), 3242–3259.

Ardhuin, F., Gualtieri, L., & Stutzmann, E., 2015. How ocean waves rock the earth: two mechanisms explain seismic noise with periods 3 to 300 s, *Geophys. Res. Lett.*, **42**, 765–772.

Ardhuin, F., Gualtieri, L., & Stutzmann, E., 2019. Physics of ambient noise generation by ocean waves, in *Surface waves and fluxes*, eds Nakata, N., Gualtieri, L., & Fichtner, A., Cambridge University Press.

Assink, J., Pichon, A. L., Blanc, E., Kallel, M., & Khemiri, L., 2014. Evaluation of wind and temperature profiles from ecmwf analysis on two hemispheres using volcanic infrasound, *Journal of Geophysical Research: Atmospheres*, **119**(14), 8659–8683.

Benioff, H. & Gutemberg, B., 1939. Waves anc currents recorded by electromagnetic barographs, *Bull. Seismol. Soc. Am.*, **20**(10), 421–426.

Blanc, E., Ceranna, L., Hauchecorne, A., Charlton-Perez, A., Marchetti, E., Evers, L. G., Kvaerna, T., Lastovicka, J., Eliasson, L., Crosby, N. B., et al., 2018. Toward an improved representation of middle atmospheric dynamics thanks to the arise project, *Surveys in geophysics*, **39**(2), 171–225.

Bowman, D. C. & Lees, J. M., 2018. Upper atmosphere heating from ocean-generated acoustic wave energy, *Geophys. Res. Lett.*, **45**, 5144–5150.

Brekhovskikh, L. M., Goncharov, V. V., Kurtepov, V. M., & Naugolnykh, K. A., 1973. The radiation of infrasound into the atmosphere by surface waves in the ocean, *Izv. Atmos. Ocean.*

Phys., **9**, 899–907 (In the English translation, 511–515.).

Bromirski, P. D., Flick, R. E., & Graham, N., 1999. Ocean wave height determined from inland seismometer data: implications for investigating wave climate changes in the NE Pacific, *J. Geophys. Res.*, **104**(C9), 20753–20766.

Ceranna, L., Matoza, R., Hupe, P., Le Pichon, A., & Landès, M., 2019. Systematic array processing of a decade of global ims infrasound data, in *Infrasound Monitoring for Atmospheric Studies*, pp. 471–482, Springer.

Cox, C. S. & Jacobs, D. C., 1989. Cartesian diver observations of double frequency pressure fluctuations in the upper levels of the ocean, *Geophys. Res. Lett.*, **16**(8), 807–810.

Donn, W. L. & Naini, B., 1973. Sea wave origin of microbaroms and microseism, *J. Geophys. Res.*, **78**(21), 4482–4488.

Donn, W. L. & Rind, D., 1971. Natural infrasound as an atmospheric probe, *Geophys. J. R. Astron. Soc.*, **26**(1), 111–133.

Drob, D., 2019. Meteorology, climatology, and upper atmospheric composition for infrasound propagation modeling, in *Infrasound Monitoring for Atmospheric Studies*, pp. 485–508, Springer.

Drob, D. P., Meier, R., Picone, J. M., & Garcés, M. M., 2010. Inversion of infrasound signals for passive atmospheric remote sensing, in *Infrasound monitoring for atmospheric studies*, pp. 701–731, Springer.

Farrell, W. E. & Munk, W., 2008. What do deep sea pressure fluctuations tell about short surface waves?, *Geophys. Res. Lett.*, **35**(7), L19605.

Garcés, M., Drob, D. P., & Picone, J. M., 2002. A theoretical study of the effect of geomagnetic fluctuations andsolar tides on the propagation of infrasonic waves in the upperatmosphere, *Geophys. J. Int.*, **148**, 77–87.

Gualtieri, L., Stutzmann, E., Farra, V., Capdeville, Y., Schimmel, M., Ardhuin, F., & Morelli, A., 2014. Modelling the ocean site effect on seismic noise body waves, *Geophys. J. Int.*, **193**, 1096–1106.

Hasselmann, K., 1962. On the non-linear energy transfer in a gravity wave spectrum, part 1:

general theory, *J. Fluid Mech.*, **12**, 481–501.

Hasselmann, K., 1963. A statistical analysis of the generation of microseisms, *Rev. of Geophys.*, **1**(2), 177–210.

Hasselmann, K., 1966. Feynman diagrams and interaction rules of wave-wave scattering processes, *Rev. of Geophys.*, **4**(1), 1–32.

Landès, M., Hubans, F., Shapiro, N. M., Paul, A., & Campillo, M., 2010. Origin of deep ocean microseisms by using teleseismic body waves, *J. Geophys. Res.*, **115**, B05302.

Le Pichon, A., Assink, J., Heinrich, P., Blanc, E., Charlton-Perez, A., Lee, C. F., Keckhut, P., Hauchecorne, A., Rüfenacht, R., Kämpfer, N., et al., 2015. Comparison of co-located independent ground-based middle atmospheric wind and temperature measurements with numerical weather prediction models, *Journal of Geophysical Research: Atmospheres*, **120**(16), 8318–8331.

Longuet-Higgins, M. S., 1950. A theory of the origin of microseisms, *Phil. Trans. Roy. Soc. London A*, **243**, 1–35.

Marty, J., 2019. The ims infrasound network: current status and technological developments, in *Infrasound Monitoring for Atmospheric Studies*, pp. 3–62, Springer.

Meschede, M., Stutzmann, E., Farra, V., Schimmel, M., & Ardhuin, F., 2017. The effect of water-column resonance on the spectra of secondary microseism p-waves, *J. Geophys. Res.*, **122**, 8121–8142.

Obrebski, M., Ardhuin, F., Stutzmann, E., & Schimmel, M., 2012. How moderate sea states can generate loud seismic noise in the deep ocean, *Geophys. Res. Lett.*, **39**, L11601.

Obrebski, M., Ardhuin, F., Stutzmann, E., & Schimmel, M., 2013. Detection of microseismic compressional (p) body waves aided by numerical modeling of oceanic noise sources, *J. Geophys. Res.*, **118**, 4312–4324.

Posmentier, E., 1967. A theory of microbaroms, *Geophys. J. R. Astron. Soc.*, **13**, 487–501.

Rascle, N. & Ardhuin, F., 2013. A global wave parameter database for geophysical applications. part 2: model validation with improved source term parameterization, *Ocean Modelling*, **70**, 174–188.

Smets, P. S. M. & Evers, L. G., 2014. The life cycle of a sudden stratospheric warming from infrasonic ambient noise observations, *J. Geophys. Res.*, **119**, 12,084–12,099.

Stutzmann, E., Schimmel, M., & Ardhuin, F., 2012. Modeling long-term seismic noise in various environments, *Geophys. J. Int.*, **191**, 707–722.

The WAVEWATCH III ® Development Group, 2016. User manual and system documentation of WAVEWATCH III ® version 5.16, Tech. Note 329, NOAA/NWS/NCEP/MMAB, College Park, MD, USA, 326 pp. + Appendices.

Waxler, R. & Assink, J., 2019. Propagation modeling through realistic atmosphere and benchmarking, in *Infrasound Monitoring for Atmospheric Studies*, pp. 509–549, Springer.

Waxler, R. & Gilbert, K. E., 2006. The radiation of atmospheric microbaroms by ocean waves, *J. Acoust. Soc. Amer.*, **119**, 2651–2664.

Waxler, R., Gilbert, K., Talmadge, C., & Hetzer, C., 2007. The effects of finite depth of the ocean on microbarom signals, in *8th International Conference on Theoretical and Computational Acoustics (ICTCA), Crete, Greece*.

APPENDIX A: GREEN FUNCTION PHASE, SPATIAL CORRELATIONS AND TREATMENT BY WAXLER AND GILBERT, 2006

In order to clarify the difference between our derivation and the derivation by (Waxler & Gilbert, 2006), we go back to their expression of the atmospheric pressure spectrum as recorded at the horizontal position $\mathbf{x}_H$ and vertical altitude z, from a collection of sources over positions y and y' in domain S. The variance of pressure is given by their eq. (49) with $\mathbf{x}'_H = \mathbf{x}_H$, $z' = z$ and $\tau = 0$

$$\left\langle P^2 \right\rangle = \rho^2 \int_{-\infty}^{\infty} \int_{-\infty}^{\infty} \int_S \int_S \langle G(x, y, -\tau_1) G^*(x, y', \tau - \tau_2) \rangle \left\langle \frac{\partial v(y, \tau_1)}{\partial \tau_1} \frac{\partial v(y', \tau_2)}{\partial \tau_2} \right\rangle_S d^2y d^2y' d\tau_1 d\tau_2 \tag{A.1}$$

Following their derivation, we use the Fourier in time $\widehat{G}$ of the Green's function, representing the propagation of acoustic waves in a layered medium as a sum of discrete modes. As given by Waxler & Gilbert (2006)[, eq. 65] the Fourier transform of the Green function for mode j and

frequency ν is given by,

$$\widehat{G}(\mathbf{x}_H, z, \mathbf{y}_H, \nu) = f(r, z) \sum_j \frac{\mathrm{e}^{\mathrm{i}k_j|\mathbf{x}_H - \mathbf{y}_H|}}{\sqrt{k_j}} \psi_j(z)\psi_j(z'), \tag{A.2}$$

where $r = |\mathbf{x}_H - \mathbf{y}_H|$ is the horizontal distance, the k_j are the horizontal wavenumbers pointing in the direction of $\widehat{\mathbf{k}} = (\mathbf{x}_H - \mathbf{y}_H)/r$, and ψ_j are normal modes satisfying the bi-orthogonality condition and their phases are assumed to be uniformly distributed and statistically independent.

Considering that for each y in the source $|\mathbf{y}'_H - \mathbf{y}_0|/|\mathbf{x}_H - \mathbf{y}_0| << 1$ with y_0 the center of the source (i.e. the receptor is far from the source), and defining the vector $\mathbf{k}_j = k_j\widehat{\mathbf{k}}$, the product of the Green's function for $\mathbf{y}_H$ and its complex conjugate for $\mathbf{y}'_H$ writes

$$\widehat{G}(\mathbf{x}_H, z, \mathbf{y}_H, \nu)\widehat{G}(\mathbf{x}_H, z, \mathbf{y}'_H, \nu)^\star = |f(r_0, z)|^2 \sum_j \mathrm{e}^{\mathrm{i}\mathbf{k}_j\cdot(\mathbf{y}'-\mathbf{y})} \frac{|\psi_j(z)|^2|\psi_j(z')|^2}{k_j} \tag{A.3}$$

The phase of this product then contains the phase shift of the propagation from $\mathbf{y}$ to $\mathbf{y}'$ with a wavenubmer k_j. When correlated with the source structure, that contains a phase $\exp[\mathrm{i}(\mathbf{k}+\mathbf{q})\cdot(\mathbf{y}'-\mathbf{y})]$ it gives,

$$\begin{aligned}
\left\langle P^2 \right\rangle &= \rho^2 \int_S \int_S \left(|f(r_0, z)|^2 \sum_j \frac{e^{i\mathbf{k_j}(\mathbf{y}'-\mathbf{y})}}{|k_j|} |\psi_j(z)|^2|\psi_j(z')|^2 \right) \\
&\quad \times \left(2 \int\int \nu^2 F(\mathbf{k})F(\mathbf{q})|C^+|^2|\Omega|^2 e^{i(\mathbf{k}+\mathbf{q})(y-y')} d^2\mathbf{k}d^2\mathbf{q} \right) d^2y d^2y' \\
&= \rho^2 \int_S \int_S |f(r_0, z)|^2 \sum_j \int\int \left[\frac{|\psi_j(z)|^2|\psi_j(z')|^2}{|k_j|} e^{i(\mathbf{k_j}-(\mathbf{k}+\mathbf{q}))(\mathbf{y}'-\mathbf{y})} \right. \\
&\quad \left. \times 2\nu^2 F(\mathbf{k})F(\mathbf{q})|C^+|^2|\Omega|^2 \right] d^2\mathbf{k}d^2\mathbf{q}d^2y d^2y'
\end{aligned}$$

This can be simplified as the integral over $\mathbf{y}'$ in the the source area S gives a term proportional to

$$\int_S \int_S \mathrm{e}^{\mathrm{i}\left[(\mathbf{k}_j-(\mathbf{k}+\mathbf{q}))\cdot(\mathbf{y}_H-\mathbf{y}'_H)\right]} d^2y d^2y' = (2\pi)^2\delta(\mathbf{k_j} - (\mathbf{k}+\mathbf{q}))S \tag{A.4}$$

instead of the $(2\pi)^2\delta(\mathbf{k}+\mathbf{q})$ term found by Waxler & Gilbert (2006).

The pressure variance becomes

$$\left\langle P^2 \right\rangle = \rho^2(2\pi)^2\, S|f(r_0, z)|^2 \sum_j \int_{\mathbf{k}+\mathbf{q}=\mathbf{k_j}} \frac{|\psi_j(z)|^2|\psi_j(z')|^2}{|k_j|} 2\,\nu^2 F(\mathbf{k})F(\mathbf{q})|C^+|^2|\Omega|^2 d^2\mathbf{k}d^2\mathbf{q}.$$

This is the same as eq. (51) in Waxler & Gilbert (2006), except for the fact that we did not replace $\mathbf{q}$ with $-\mathbf{k}$, we thus need to compute the the air pressure over the source for all $\mathbf{K} = \mathbf{k_j}$. Although

667 $|\mathbf{K}| \ll |\mathbf{k}|$, the approximation $|\mathbf{K}| = \mathbf{0}$, which is only strictly valid for an azimuth angle $\theta_a = 0$,

668 leads to very large differences in the source amplitude, up to 30 dB as shown in figure 3.

submitted to *Geophys. J. Int.*

Supporting Information for "Atmospheric infrasound radiation from ocean waves in finite depth: a unified generation theory and application to radiation patterns"

M. De Carlo[1, 2], F. Ardhuin[2], A. Le Pichon[1]

[1] *CEA, DAM, DIF, F-91297, Arpajon, France;* [2] *Univ. Brest, CNRS, IRD, Ifremer, Laboratoire d'Océanographie Physique et Spatiale (LOPS), IUEM, Brest, France*

10 October 2019

This document presents all the details of derivations necessary to support the paper "Atmospheric infrasound radiation from ocean waves in finite depth: a unified generation theory and application to radiation patterns". It follow Brekhovskikh et al. (1973, hereinafter BGKN73), as much as possible. Because we use the more common convention that the velocity vector is $\mathbf{v} = \nabla\phi$ this leads to changes in signs that are highlighted in red. A notable difference with Waxler & Gilbert (2006, hereinafter WG06) is the non-zero value of $\mathbf{k}\cdot\mathbf{k}' + kk'$ and similar terms. Some of these were obtained by WG06 using the divergence equation, but not all of them, which misses the azimuthal dependence of the solution.

For convenience we repeat in table 1 the list of notations from the paper, including a few more symbols that were not used in the paper.

S1 EQUATIONS UP TO EQ. (9) IN BGKN73

We start with the Euler equations for a perfect fluid (no viscosity),

$$\rho_j\big(\frac{\partial \mathbf{v}_j}{\partial t} + (\mathbf{v}_j \cdot \nabla)\mathbf{v}_j\big) = -\nabla p_j - g\rho_j \nabla z \tag{S1}$$

Table S1. Notations used in different papers: LH50 stands for (Longuet-Higgins, 1950), BGKN73 stands for (Brekhovskikh et al., 1973), WG06 stands for (Waxler & Gilbert, 2006) and AH13 stands for (Ardhuin & Herbers, 2013).

quantity	this paper	LH50	BGKN73	WG06	AH13
vertical coordinate	z	$-z$	z	z	z
angle relative to vertical	θ_a or θ_w	–	θ	–	–
surface elevation	ζ	ζ	ζ	ξ	ζ
azimuth of spectrum	φ	θ	φ	θ	θ
azimuth of acoustic signal	θ_2	–	φ_a	–	–
velocity potential	ϕ	$-\phi$	$-\varphi$	ϕ	ϕ
layer index	l	–	j	σ	–
sound speed	α_l	c	c_j	c_σ	α
density ratio	m	–	m	–	–
horizontal wavenumber	$\mathbf{K}$	–	$\mathbf{q}$	–	$\mathbf{K}$
radian frequency	Ω	–	Ω	–	$2\pi f_s$
horizontal wavenumbers	$\mathbf{k}$, $\mathbf{k}'$	$(-uk, -vk)$	$\varkappa$, $\varkappa_1$	$\mathbf{k}$, $\mathbf{q}$	$\mathbf{k}$, $\mathbf{k}'$
radian frequencies	$\sigma\sigma'$	σ	$\omega(\varkappa)$,$\omega(\varkappa_1)$	$\omega(\mathbf{k})$,$\omega(\mathbf{q})$	$\sigma\sigma'$
pressure	p	p	$\rho\mathcal{P}$	p	p
vertical wavenumbers	$\nu_\pm$, $\mu_\pm$	$-$, α	λ_1,λ_2	–	l_a, l
upward amplification	$g/2\alpha_l$	γ	–	–	–

We then use the compressible form of the Bernoulli Equation. And the mass conservation.

$$\frac{\partial \rho_j}{\partial t} + \nabla(\rho_j \mathbf{v}_j) = 0 \tag{S2}$$

We do not repeat here the equations (1) to (6) from BGKN73.

S1.1 About equation (1) in BGKN73

Eq. (S1) can be rewritten as

$$\begin{aligned}(\rho_0 \;+\; s\rho_1 + s^2\rho_2)\left(\frac{\partial s\mathbf{v}_1 + s^2\mathbf{v}_2}{\partial t} + (s\mathbf{v}_1 + s^2\mathbf{v}_2)\cdot\nabla(s\mathbf{v}_1 + s^2\mathbf{v}_2)\right)\\ = \;-\nabla(p_0 + sp_1 + s^2p_2) - g(\rho_0 + s\rho_1 + s^2\rho_2)\nabla z.\end{aligned} \tag{S3}$$

Its truncation at the different orders in wave slope give,

• Order 0,

$$-\nabla p_0 = g\rho_0 \nabla z \tag{S4}$$

• Order 1,

$$\rho_0 \frac{\partial \mathbf{v}_1}{\partial t} + 0 = -\nabla p_1 - g\rho_1 \nabla z$$

However (eq 6) : $\nabla p_1 = \nabla(\rho_0 \mathcal{P}_1) = \mathcal{P}_1 \nabla(\rho_0) + \rho_0 \nabla(\mathcal{P}_1) = \mathcal{P}_1 \rho_0 \cdot \frac{-g}{\alpha^2} \nabla z + \rho_0 \nabla(\mathcal{P}_1) = \frac{\alpha^2 \rho_1}{\rho_0} \cdot \rho_0 \cdot \frac{-g}{\alpha^2} \nabla z + \rho_0 \nabla(\mathcal{P}_1)$.

Equation (S3) for order 1 becomes

$$\frac{\partial \mathbf{v}_1}{\partial t} + \nabla \mathcal{P}_1 = 0. \tag{S5}$$

• Order 2:

$$\rho_0 \frac{\partial \mathbf{v}_2}{\partial t} + \rho_1 \frac{\partial \mathbf{v}_1}{\partial t} + \rho_0 \mathbf{v}_1 \nabla \mathbf{v}_1 = -\nabla p_2 - g\rho_2 \nabla z \tag{S6}$$

We similarly obtain

$$\begin{aligned} -\nabla p_2 - g\rho_2 \nabla z &= -\nabla(\rho_0 \mathcal{P}_2) - g\rho_2 \nabla z = -\rho_0 \nabla(\mathcal{P}_2) - \alpha^2 \frac{\rho_2}{\rho_0} \nabla(\rho_0) - g\rho_2 \nabla z \\ &= -\rho_0 \nabla(\mathcal{P}_2) - \alpha^2 \frac{\rho_2}{\rho_0} \cdot \frac{-g}{\alpha^2} \nabla z - g\rho_2 \nabla z = -\rho_0 \nabla(\mathcal{P}_2). \end{aligned}$$

Then,

$$\frac{\partial \mathbf{v}_2}{\partial t} + \frac{\rho_1}{\rho_0} \frac{\partial \mathbf{v}_1}{\partial t} + \mathbf{v}_1 \nabla \mathbf{v}_1 = -\nabla \mathcal{P}_2.$$

Remembering from order 1 that $\frac{\partial \mathbf{v}_1}{\partial t} = -\nabla \mathcal{P}_1$, one obtains

$$\begin{aligned} \frac{\partial \mathbf{v}_2}{\partial t} + \nabla \mathcal{P}_2 &= -\frac{\rho_1}{\rho_0} \frac{\partial \mathbf{v}_1}{\partial t} - \mathbf{v}_1 \nabla \mathbf{v}_1 = \frac{\rho_1 \alpha^2}{\rho_0 \alpha^2} \nabla \mathcal{P}_1 - \mathbf{v}_1 \nabla \mathbf{v}_1 \\ &= \frac{1}{\alpha^2} \mathcal{P}_1 \nabla \mathcal{P}_1 - \mathbf{v}_1 \nabla \mathbf{v}_1 = \frac{1}{2} \nabla \left(\frac{\mathcal{P}_1^2}{\alpha^2} - \mathbf{v}_1^2 \right) + \mathbf{v}_1 \times \mathbf{rot} \mathbf{v}_1 \end{aligned}$$

Because the velocity field is irrotational, it can be expressed as the gradient of a potential velocity ϕ,

$$\mathbf{v}_i = +\nabla \phi. \tag{S7}$$

This gives,

$$\nabla \mathcal{P}_1 = -\frac{\partial \nabla \phi_1}{\partial t}$$
$$\nabla \mathcal{P}_2 = -\frac{\partial \nabla \phi_2}{\partial t} + \frac{1}{2}\nabla\left(\frac{\mathcal{P}_1^2}{\alpha^2} - (\nabla\phi_1)^2\right)$$

Which can also be written

$$\mathcal{P}_1 = -\frac{\partial \phi_1}{\partial t} \tag{S8}$$
$$\mathcal{P}_2 = -\frac{\partial \phi_2}{\partial t} + \left(\frac{\mathcal{P}_1^2}{2\alpha^2} - \frac{(\nabla\phi_1)^2}{2}\right). \tag{S9}$$

S1.2 About equation (2) in BGKN73 and the acoustic wave equation

• Order 1:

$$\begin{aligned} & \frac{\partial \rho_1}{\partial t} + \nabla(\rho_0 \mathbf{v}_1) = 0 \\ \iff \quad & \frac{\partial \rho_1}{\partial t} + \rho_0 \nabla \mathbf{v}_1 + \mathbf{v}_1 \nabla \rho_0 = 0 \\ \iff \quad & \frac{\partial \rho_1}{\partial t} = -\rho_0 \Delta \phi_1 - \nabla\phi_1 \nabla \rho_0 \end{aligned} \tag{S10}$$

$\frac{\partial}{\partial t}\big(\rho_0 \cdot (6)\big) - \alpha^2 \cdot (8)$ leads to

$$\begin{aligned} & \frac{\partial \rho_0 \mathcal{P}_1}{\partial t} - \alpha^2 \frac{\partial \rho_1}{\partial t} - \alpha^2 \rho_0 \Delta\phi_1 - \alpha^2 \nabla\phi_1 \nabla\rho_0 = -\frac{\partial^2 \rho_0 \phi_1}{\partial t^2} \\ \iff & \frac{\partial p_1}{\partial t} - \alpha^2 \frac{\partial \alpha^{-2} p_1}{\partial t} - \alpha^2 \rho_0 \Delta\phi_1 + \alpha^2 \nabla\phi_1 \rho_0 \frac{g}{\alpha^2}\nabla z = -\rho_0 \frac{\partial^2 \phi_1}{\partial t^2} \\ \iff & -\alpha^2 \Delta\phi_1 + g\frac{\partial \phi_1}{\partial z} + \frac{\partial^2 \phi_1}{\partial t^2} = 0 \\ \iff & \Delta\phi_1 - \frac{g}{\alpha^2}\frac{\partial \phi_1}{\partial z} - \frac{1}{\alpha^2}\frac{\partial^2 \phi_1}{\partial t^2} = 0 \end{aligned} \tag{S11}$$

And we retrieve the two equations of system (9) in BGKN73.

• Order 2:

$$\begin{aligned} & \frac{\partial \rho_2}{\partial t} + \nabla(\rho_0 \mathbf{v}_2 + \rho_1 \mathbf{v}_1) = 0 \\ \iff \quad & \frac{\partial \rho_2}{\partial t} + \rho_0 \nabla \mathbf{v}_2 + \mathbf{v}_2 \nabla \rho_0 + \rho_1 \nabla \mathbf{v}_1 + \mathbf{v}_1 \nabla \rho_1 = 0 \\ \iff \quad & \frac{\partial \rho_2}{\partial t} = -\rho_0 \Delta \phi_2 - \nabla\phi_2 \nabla \rho_0 - \rho_1 \Delta\phi_1 - \nabla\phi_1 \nabla\rho_1 \end{aligned} \tag{S12}$$

$\frac{\partial}{\partial t}\left(\rho_0 \cdot (7)\right) - \alpha^2 \cdot (10)$ leads to:

$$\frac{\partial \rho_0 \mathcal{P}_2}{\partial t} - \alpha^2 \frac{\partial \rho_2}{\partial t} - \alpha^2 \rho_0 \Delta\phi_2 - \alpha^2 \nabla\phi_2 \nabla\rho_0 - \alpha^2 \rho_1 \Delta\phi_1 - \alpha^2 \nabla\phi_1 \nabla\rho_1 = -\frac{\partial^2 \rho_0 \phi_2}{\partial t^2} + \rho_0 \frac{\partial}{\partial t}\left(\frac{\mathcal{P}_1^2}{2\alpha^2} - \frac{(\nabla\phi_1)^2}{2}\right)$$

$$\iff \frac{\partial p_2}{\partial t} - \alpha^2 \frac{\partial \alpha^{-2} p_2}{\partial t} - \alpha^2 \rho_0 \Delta\phi_2 + \alpha^2 \rho_0 \frac{g}{\alpha^2}\frac{\partial \phi_2}{\partial z} - p_1 \Delta\phi_1 - \nabla\phi_1 \nabla p_1 = -\rho_0 \frac{\partial^2 \phi_2}{\partial t^2} + \rho_0 \frac{\partial}{\partial t}\left(\frac{\mathcal{P}_1^2}{2\alpha^2} - \frac{(\nabla\phi_1)^2}{2}\right)$$

$$\iff -\alpha^2 \rho_0 \Delta\phi_2 + \alpha^2 \rho_0 \frac{g}{\alpha^2}\frac{\partial \phi_2}{\partial z} - \rho_0 \mathcal{P}_1 \Delta\phi_1 - \mathcal{P}_1 \nabla\phi_1 \nabla\rho_0 - \rho_0 \nabla\phi_1 \nabla\mathcal{P}_1 = -\rho_0 \frac{\partial^2 \phi_2}{\partial t^2} + \rho_0 \frac{\partial}{\partial t}\left(\frac{\mathcal{P}_1^2}{2\alpha^2} - \frac{(\nabla\phi_1)^2}{2}\right)$$

$$\iff -\alpha^2 \rho_0 \Delta\phi_2 + \rho_0 g \frac{\partial \phi_2}{\partial z} - \rho_0 \mathcal{P}_1 \Delta\phi_1 + \mathcal{P}_1 \rho_0 \frac{g}{\alpha^2}\frac{\partial \phi_1}{\partial z} - \rho_0 \nabla\phi_1 \nabla\mathcal{P}_1 = -\rho_0 \frac{\partial^2 \phi_2}{\partial t^2} + \rho_0 \frac{\partial}{\partial t}\left(\frac{\mathcal{P}_1^2}{2\alpha^2} - \frac{(\nabla\phi_1)^2}{2}\right)$$

$$\iff -\alpha^2 \rho_0 \Delta\phi_2 + \rho_0 g \frac{\partial \phi_2}{\partial z} - \rho_0 \mathcal{P}_1 \left(\Delta\phi_1 - \frac{g}{\alpha^2}\frac{\partial \phi_1}{\partial z}\right) - \rho_0 \nabla\phi_1 \nabla\mathcal{P}_1 = -\rho_0 \frac{\partial^2 \phi_2}{\partial t^2} + \rho_0 \frac{\partial}{\partial t}\left(\frac{\mathcal{P}_1^2}{2\alpha^2} - \frac{(\nabla\phi_1)^2}{2}\right)$$

$$\iff -\alpha^2 \rho_0 \Delta\phi_2 + \rho_0 g \frac{\partial \phi_2}{\partial z} - \rho_0 \mathcal{P}_1 \frac{1}{\alpha^2}\frac{\partial^2 \phi_1}{\partial t^2} - \rho_0 \nabla\phi_1 \nabla\mathcal{P}_1 = -\rho_0 \frac{\partial^2 \phi_2}{\partial t^2} + \rho_0 \frac{\partial}{\partial t}\left(\frac{\mathcal{P}_1^2}{2\alpha^2} - \frac{(\nabla\phi_1)^2}{2}\right)$$

$$\iff -\alpha^2 \rho_0 \Delta\phi_2 + \rho_0 g \frac{\partial \phi_2}{\partial z} + \rho_0 \mathcal{P}_1 \frac{1}{\alpha^2}\frac{\partial \mathcal{P}_1}{\partial t} - \rho_0 \nabla\phi_1 \nabla\mathcal{P}_1 = -\rho_0 \frac{\partial^2 \phi_2}{\partial t^2} + \rho_0 \frac{\partial}{\partial t}\left(\frac{\mathcal{P}_1^2}{2\alpha^2} - \frac{(\nabla\phi_1)^2}{2}\right)$$

$$\iff -\alpha^2 \rho_0 \Delta\phi_2 + \rho_0 g \frac{\partial \phi_2}{\partial z} + \rho_0 \nabla\phi_1 \nabla \frac{\partial \phi_1}{\partial t} = -\rho_0 \frac{\partial^2 \phi_2}{\partial t^2} - \rho_0 \frac{\partial}{\partial t}\frac{(\nabla\phi_1)^2}{2}$$

$$\iff -\alpha^2 \rho_0 \Delta\phi_2 + \rho_0 g \frac{\partial \phi_2}{\partial z} + \rho_0 \frac{\partial}{\partial t}\frac{(\nabla\phi_1)^2}{2} = -\rho_0 \frac{\partial^2 \phi_2}{\partial t^2} - \rho_0 \frac{\partial}{\partial t}\frac{(\nabla\phi_1)^2}{2}$$

$$\iff -\alpha^2 \rho_0 \Delta\phi_2 + \rho_0 g \frac{\partial \phi_2}{\partial z} + \rho_0 \frac{\partial^2 \phi_2}{\partial t^2} = -\rho_0 \frac{\partial}{\partial t}(\nabla\phi_1)^2$$

$$\iff \Delta\phi_2 - \frac{g}{\alpha^2}\frac{\partial \phi_2}{\partial z} - \frac{1}{\alpha^2}\frac{\partial^2 \phi_2}{\partial t^2} = +\frac{1}{\alpha^2}\frac{\partial}{\partial t}(\nabla\phi_1)^2 \tag{S13}$$

S1.3 About Boundary conditions

We use the same boundary conditions as in BGKN73 for $z = 0$ for velocity,

$$-\left.\frac{\partial \phi_1}{\partial z}\right|_{z=0} + \frac{\partial \zeta_1}{\partial t} = 0 \tag{S14}$$

$$-\left.\frac{\partial \phi_2}{\partial z}\right|_{z=0} + \frac{\partial \zeta_2}{\partial t} = -\left(-\left.\frac{\partial^2 \phi_1}{\partial z^2}\right|_{z=0} \zeta_1 + \nabla\phi_1|_{z=0} \nabla\zeta_1\right) \tag{S15}$$

And for pressure,

$$(\mathcal{P}_{w,1} - m\mathcal{P}_{a,1})_{z=0} - g(1-m)\zeta_1 = 0 \tag{S16}$$

$$(\mathcal{P}_{w,2} - m\mathcal{P}_{a,2})_{z=0} - g(1-m)\zeta_2 = -\left(\frac{\partial \mathcal{P}_{w,1}}{\partial z} - m\frac{\partial \mathcal{P}_{a,1}}{\partial z}\right)_0 \zeta_1$$

$$+\frac{g}{\alpha_a^2}(n^2 \mathcal{P}_{w,1} - m\mathcal{P}_{a,1})_0 \zeta_1 - \frac{g^2}{2\alpha_a^2}(n^2 - m^2)\zeta_1^2 \tag{S17}$$

Here is a summary of the system of equation that corresponds to eq. (9) in BGKN73

$$\Delta\phi_{j,i} - \frac{g}{\alpha_j^2}\frac{\partial\phi_{j,i}}{\partial z} - \frac{1}{\alpha_j^2}\frac{\partial^2\phi_{j,i}}{\partial t^2} = S_{j,i} \qquad \mathcal{P}_{j,i} = -\frac{\partial\phi_{j,i}}{\partial t} + F_{j,i}$$

$$-\left.\frac{\partial\phi_{j,i}}{\partial z}\right|_{z=0} + \frac{\partial\zeta_i}{\partial t} = Q_{j,i} \qquad (\mathcal{P}_{w,i} - m\mathcal{P}_{a,i})_{z=0} - g(1-m)\zeta_i = R_i$$

where,

$$F_{j,1} = S_{j,1} = Q_{j,1} = R_1 = 0$$

$$F_{j,2} = \frac{\mathcal{P}_{j,1}^2}{2\alpha_j^2} - \frac{(\nabla\phi_{j,1})^2}{2}, \qquad S_{j,2} = +\frac{1}{\alpha_j^2}\frac{\partial}{\partial t}(\nabla\phi_{j,1})^2$$

$$Q_{j,2} = -\nabla\phi_{j,1}|_0\nabla\zeta_1 + \left.\frac{\partial^2\phi_{j,1}}{\partial z^2}\right|_{z=0}\zeta_1$$

$$R_2 = -\left(\frac{\partial\mathcal{P}_{w,1}}{\partial z} - m\frac{\partial\mathcal{P}_{a,1}}{\partial z}\right)_0\zeta_1 + \frac{g}{\alpha_a^2}(n^2\mathcal{P}_{w,1} - m\mathcal{P}_{a,1})_0\zeta_1 - \frac{g^2}{2\alpha_a^2}(n^2-m^2)\zeta_1^2$$

$$m = \rho_{a,0}/\rho_{w,0}, \qquad n = \alpha_a/\alpha_w, \qquad \delta_a = \left(\frac{g}{\alpha_a^2 k}\right)^{1/2} = \frac{\sigma}{\alpha_a k}, \qquad \delta_w = n\delta_a$$

S2 SOLVING FOR FIRST ORDER AND EXPRESSING THE SECOND ORDER PROBLEM

S2.1 First order

By Fourier transform in horizontal space and time we can take

$$\phi_{j,1} = -\mathrm{i}s\sigma\sum\Phi_{j,1}(z)Z\mathrm{e}^{\mathrm{i}(\mathbf{k}\cdot\mathbf{x}-s\sigma t)} \tag{S18}$$

The boundary condition in $z = 0$ leads to

$$\Phi_{j,1}(z=0) = 1. \tag{S19}$$

Assuming $\Phi_{j,1}(z) = f_j(z)\mathrm{e}^{\gamma_j z}$ with $\gamma_j = g/2\alpha_j^2$ one obtains,

- for the air

$$\phi_{a,1} = \sum\mathrm{i}\frac{s\sigma}{k_a}\mathrm{e}^{-k_a z}Z\mathrm{e}^{\mathrm{i}(\mathbf{k}\cdot\mathbf{x}-s\sigma t)} \tag{S20}$$

with

$$\begin{aligned}
k_a &= -\gamma_a + k_{a0} \\
&= -\frac{g}{2\alpha_a^2} + \sqrt{k^2 - \gamma_a^2 + \frac{g\gamma_a}{\alpha_a^2} - \frac{\sigma^2}{\alpha_a^2}} \\
&= -\frac{g}{2\alpha_a^2} + k(1 - \frac{g^2}{4\alpha_a^4 k^2} + \frac{g^2}{2\alpha_a^4 k^2} - \frac{\sigma^2}{k^2\alpha_a^2} \\
&= -k\frac{g}{2k\alpha_a^2} + k\left(1 - \frac{\delta_a^4}{4} + \frac{\delta_a^4}{2} - \delta_a^2\right)^{1/2} \\
&= -k\frac{\delta_a^2}{2} + k\left(1 - \frac{\delta_a^2}{2}\right) \\
&= k\left(1 - \delta_a^2\right)
\end{aligned}$$

- for the water :

$$\phi_{w,1} = \sum -\mathrm{i}s\sigma \frac{k_{w0}\cosh\left(k_{w0}(z+h)\right) - \gamma_w \sinh\left(k_{w0}(z+h)\right)}{k_w^2 \sinh\left(k_{w0}h\right)} \mathrm{e}^{\gamma_w z} Z \mathrm{e}^{\mathrm{i}(\mathbf{k}\cdot\mathbf{x} - s\sigma t)} \tag{S21}$$

with $k_w^2 = k_{w0}^2 - \gamma_w^2 = k^2(1 - 2\delta_w^2)$

If we consider δ_w^2 to be negligible ($\delta_w = n^2\delta_a^2 \simeq 0.05\delta_a^2$) we obtain :

$$\phi_{w,1} = \sum -\mathrm{i}s\sigma \frac{\cosh\left(k_{w0}(z+h)\right)}{k\sinh\left(k_{w0}h\right)} \mathrm{e}^{\gamma_w z} Z \mathrm{e}^{\mathrm{i}(\mathbf{k}\cdot\mathbf{x} - s\sigma t)} \tag{S22}$$

For simplicity we will now write that :

$$\phi_{w,1} = \sum -\mathrm{i}s\sigma f_{w,k}(z) \mathrm{e}^{\gamma_w z} Z \mathrm{e}^{\mathrm{i}(\mathbf{k}\cdot\mathbf{x} - s\sigma t)} \tag{S23}$$

S2.2 Second order

At second order, the effects of waves comes into the pressure and velocity boundary conditions at the interfaces, but also as forcing terms on the right hand side of the wave equation. All these different terms take different forms, in particular for waves in intermediate or shallow water (Ardhuin & Herbers, 2013). In the limit of deep water waves, $kh \gg 1$, and neglecting δ_w^2 terms, all the wave forcing terms can be expressed as a function of $\hat{p}_{2,u}$, defined as

$$\hat{p}_{2,u}(x,y,z) = \rho_w |\nabla\phi_1|^2 = \frac{\rho_w g^2}{s\sigma s'\sigma'} \sum \left(\mathbf{k}\cdot\mathbf{k}' - kk'\right) Z Z' \mathrm{e}^{(k+k')z} \mathrm{e}^{\mathrm{i}\Theta} \tag{S24}$$

with $\Theta = \mathbf{K}\cdot\mathbf{x} - \Omega t$, $\mathbf{K} = \mathbf{k} + \mathbf{k}'$, and $\Omega = s\sigma + s'\sigma'$. A the surface, $z = 0$, this equivalent pressure, correspond to the pressure that drives microseisms as given by Hasselmann (1963, eq. 2.12).

In the following, we will neglect all the short wavelength components that correspond to the middle line of eq. (2.13) of (Hasselmann, 1963), keeping only the large wavelengths that excite microbaroms, and for which $|\mathbf{k} + \mathbf{k}'| \ll |\mathbf{k}|$.

Given that acoustic waves in the atmosphere are much slower than those in water, we will retain δ_a^2 terms. As a result, following (Brekhovskikh et al., 1973), we cannot use the approximation $\mathbf{k}\cdot\mathbf{k}' \simeq 0$, but instead, using $\mathbf{k}\cdot\mathbf{k}' < 0$ for those components that produce microseisms, we can use

$$\frac{K}{k} = \frac{K\alpha_a}{2\sigma}\frac{2\sigma}{k\alpha_a} = 2\sin\theta_a\delta_a \tag{S25}$$

and the law of cosine in triangles,

$$2\mathbf{k}\cdot\mathbf{K} = k^2 + K^2 - k'^2 \tag{S26}$$

this gives,

$$\begin{aligned}
kk' + \mathbf{k}\cdot\mathbf{k}' &= kk'\left[1 - \left(\left(\frac{-\mathbf{k}\cdot\mathbf{k}'}{kk'}\right)^2\right)^{1/2}\right] = kk'\left[1 - \left(\left(\frac{\mathbf{K}\cdot\mathbf{k}' - \mathbf{k}'\cdot\mathbf{k}'}{kk'}\right)\left(\frac{\mathbf{k}\cdot\mathbf{K} - \mathbf{k}\cdot\mathbf{k}}{kk'}\right)\right)^{1/2}\right] \\
&= kk'\left[1 - \left(\left(\frac{-\mathbf{K}\cdot\mathbf{k} + K^2 - k'^2}{kk'}\right)\left(\frac{\mathbf{k}\cdot\mathbf{K} - k^2}{kk'}\right)\right)^{1/2}\right] \\
&= kk'\left[1 - \left(\frac{k^2k'^2 - (\mathbf{K}\cdot\mathbf{k})^2 + \mathbf{K}\cdot\mathbf{k}\left(k^2 + K^2 - k'^2\right) - k^2K^2}{k^2k'^2}\right)^{1/2}\right] \\
&= kk'\left[1 - \left(1 + \frac{-(\mathbf{K}\cdot\mathbf{k})^2 + 2\mathbf{K}\cdot\mathbf{k}(\mathbf{K}\cdot\mathbf{k}) - k^2K^2}{k^2k'^2}\right)^{1/2}\right] \\
&= kk'\left[1 - \left(1 + \frac{(\mathbf{K}\cdot\mathbf{k})^2 - k^2K^2}{k^2k'^2}\right)^{1/2}\right] \\
&\simeq kk'\left[-\frac{1}{2}\left(\frac{(\mathbf{K}\cdot\mathbf{k})^2}{k^2k'^2} - \frac{K^2}{k'^2}\right)\right] \simeq kk'\frac{1}{2}\frac{K^2}{k'^2}\left[1 - \left(\frac{(\mathbf{K}\cdot\mathbf{k})^2}{k^2K^2}\right)\right] \\
&\simeq 2kk'\sin^2\theta_a\delta_a^2\left[1 - \left(\frac{(\mathbf{k}\cdot\mathbf{K})^2}{k^2K^2}\right)\right] = 2kk'\sin^2\theta_a\delta_a^2\left[1 - \cos^2(\varphi_2 - \varphi)\right]
\end{aligned} \tag{S27}$$

which is a function of the azimuth φ_2 of the acoustic wave propagation, with $\cos(\varphi_2 - \varphi) = \mathbf{k}\cdot\mathbf{K}/(kK)$.

Then,

$$\mathbf{k}\cdot\mathbf{k}' - kk' \simeq -2kk' \left(1 - \sin^2\theta_a\delta_a^2\left[1-\cos^2(\varphi_2-\varphi)\right]\right) \tag{S28}$$

This gives,

$$\hat{p}_{2,u}(x,y,z) \simeq -2\rho_w\sigma\sigma' \sum \left(1 - \sin^2\theta_a\delta_a^2\left[1-\cos^2(\varphi_2-\varphi)\right]\right) ZZ' \mathrm{e}^{(k+k')z}\mathrm{e}^{\mathrm{i}\Theta} \tag{S29}$$

Other similar terms have more simple forms with no azimuthal dependency

$$\frac{1}{2}\left(k^2 + \mathbf{k}\cdot\mathbf{k}' + k'^2 + \mathbf{k}\cdot\mathbf{k}'\right) = \frac{1}{2}\left(\mathbf{k}\cdot\mathbf{K} + \mathbf{k}'\cdot\mathbf{K}\right) = \frac{1}{2}K^2 \simeq 2k^2\sin^2\theta_a\delta_a^2. \tag{S30}$$

S3 SECOND ORDER SOLUTION

S3.1 General form of the solution in the water layer

The homogeneous solution is obtained for $S_{w,2} = 0$,

$$\phi_{w,2,h}(x,y,z,t) = \sum \Phi_{w,2,h}\mathrm{e}^{\mathrm{i}\Theta}, \quad \text{with} \quad \Theta = \mathbf{K}\cdot\mathbf{x} - \Omega t, \quad \mathbf{K} = \mathbf{k}+\mathbf{k}', \quad \Omega = s\sigma + s'\sigma' \tag{S31}$$

Assuming a $\mathrm{e}^{\mathrm{i}\mu z}$ variation over the vertical and replacing in the homogeneous equation (S13) gives,

$$\mu^2 + \mathrm{i}\frac{g}{\alpha_w^2}\mu + (K^2 - \Omega^2/\alpha_w^2) = 0 \tag{S32}$$

with solutions,

$$\mu_\pm = -\mathrm{i}\frac{g}{\alpha_w^2} \pm \sqrt{\frac{g^2}{2\alpha_w^4} + (\Omega^2/\alpha_w^2 - K^2)} \simeq \pm k_{w2,0}(1 + O(\delta_w^2)) \tag{S33}$$

with the complex wavenumber $k_{w2,0} = \sqrt{\Omega^2/\alpha_w^2 - K^2}$ so that the homogeneous solution is

$$\Phi_{w,2,h} = W_+\mathrm{e}^{\mathrm{i}\mu_+ z} + W_-\mathrm{e}^{\mathrm{i}\mu_- z}. \tag{S34}$$

We recall that the wave equation is forced by,

$$S_{w,2} = +\frac{1}{\alpha_w^2}\frac{\partial}{\partial t}\left(\nabla\phi_1\right)^2 = +\frac{1}{\rho_w\alpha^2}\frac{\partial\widehat{p}_{2,u}}{\partial t} \tag{S35}$$

This forcing adds a particular solution of order δ_w^2 that could be neglected here but we will only keep the lowest order term to be consistent with BGKN73. This is also discussed by (Longuet-Higgins, 1950) and (Waxler & Gilbert, 2006). We will only give its expression in the limit of deep water, i.e. $kh \gg 1$.

we recall the right hand side,

$$S_{w,2}(x,z,t) \simeq +\frac{1}{\rho_w \alpha_w^2}\frac{\partial \widehat{p}_{2,u}(x,y,z,t)}{\partial t} = -\frac{g^2}{\alpha_a^2}\sum \mathrm{i}\frac{s\sigma + s\sigma'}{s\sigma s\sigma'}\left(\mathbf{k}\cdot\mathbf{k}' - kk'\right) ZZ' \mathrm{e}^{(k_w+k'_w)z}\mathrm{e}^{\mathrm{i}\Theta}. \tag{S36}$$

Looking for a solution of the form

$$\phi_{w,2,p} = \sum \Phi_{w,2,p}\mathrm{e}^{\mathrm{i}\Theta}. \tag{S37}$$

we replace in the wave equation (S13) and find

$$\Phi_{w,2,p} \simeq -\mathrm{i}\frac{g^2}{u}\cdot\frac{s\sigma + s\sigma'}{s\sigma s\sigma'}\left(\mathbf{k}\cdot\mathbf{k}' - kk'\right) ZZ' \mathrm{e}^{(k_w+k'_w)z}. \tag{S38}$$

with the denominator defined by

$$u = \alpha_w^2\left[-K^2 + \frac{\Omega^2}{\alpha_w^2} + (k_w + k'_w)^2\right] + g(k_w + k'_w) \simeq \alpha_w^2(k_w + k'_w)^2 \simeq 4\alpha_w^2 k^2. \tag{S39}$$

Of particular interest is the long-wavelength part – with $s = s'$ – of the vertical derivative of $\phi_{w,2,p}$, given by,

$$\begin{aligned}\frac{\partial \phi_{w,2,p}}{\partial z} &\simeq \sum -\mathrm{i}s\frac{g^2}{4\alpha_w^2 k^2}\frac{2\sigma(k_w + k'_w)}{\sigma\sigma'}\left(\mathbf{k}\cdot\mathbf{k}' - kk'\right) ZZ' \mathrm{e}^{(k_w+k'_w)z}\mathrm{e}^{\mathrm{i}\Theta},\\ &\simeq +\sum \mathrm{i}s\delta_w^2\frac{g}{\sigma}2k^2 ZZ' \mathrm{e}^{(k_w+k'_w)z}\mathrm{e}^{\mathrm{i}\Theta}.\end{aligned} \tag{S40}$$

S3.2 General form of the solution in the air layer

For the air, we only consider here acoustic waves radiating upward, giving the homogeneous solution,

$$\phi_{a,2,h}(x,y,z,t) = \sum sA_+ ZZ' \mathrm{e}^{\nu_+ z}\mathrm{e}^{\mathrm{i}\Theta}, \tag{S41}$$

where

$$\nu_+ = \frac{g}{\alpha_a^2} + \mathrm{i}\sqrt{\frac{g^2}{2\alpha^4} + (\Omega^2/\alpha_w^2 - K^2)}. \tag{S42}$$

For the particular solution, we recall the right hand side,

$$S_{a,2}(x,z,t) \simeq +\frac{1}{\rho_w \alpha_a^2}\frac{\partial \widehat{p}_{2,u}(x,y,-z,t)}{\partial t} = -\frac{g^2}{\alpha_a^2}\sum \mathrm{i}\frac{s\sigma + s\sigma'}{s\sigma s\sigma'}\left(\mathbf{k}\cdot\mathbf{k}' - k_a k'_a\right) ZZ' \mathrm{e}^{-(k_a+k'_a)z}\mathrm{e}^{\mathrm{i}\Theta}. \tag{S43}$$

Looking for a solution of the form

$$\phi_{a,2,p} = \sum \Phi_{a,2,p} \mathrm{e}^{\mathrm{i}\Theta}. \tag{S44}$$

we replace in the wave equation (S13) and find

$$\Phi_{a,2,p} \simeq -\mathrm{i}\frac{g^2}{u}\frac{s\sigma + s\sigma'}{s\sigma s\sigma'}\left(\mathbf{k}\cdot\mathbf{k}' - k_a k'_a\right) Z Z' \mathrm{e}^{-(k_a+k'_a)z}. \tag{S45}$$

with the denominator defined by

$$u = \alpha_a^2\left[-K^2 + \frac{\Omega^2}{\alpha_a^2} + (k_a + k'_a)^2\right] + g(k_a + k'_a) \simeq \alpha_a^2(k_a + k'_a)^2 \simeq 4\alpha_a^2 k^2. \tag{S46}$$

$$\begin{aligned} u &= \alpha_a^2\left[-K^2 + \frac{\Omega^2}{\alpha_a^2} + (k_a + k'_a)^2\right] + g(k_a + k'_a) \\ &\simeq \alpha_a^2 k^2\left(4\delta_a^2\cos^2\theta_a + \left(1 + \frac{k'}{k}\right)^2(1 - 2\delta_a^2) + \frac{g}{\alpha_a^2 k^2}(k_a + k'_a)\right) \\ &\simeq \alpha_a^2 k^2(4\delta_a^2\cos^2\theta_a + 4(1 - 2\delta_a^2) + 2\delta_a^2(1 - \delta_a^2)) \\ &\simeq 4\alpha_a^2 k^2(1 - \delta_a^2(\sin^2\theta_a + \frac{1}{2})) \simeq 4\alpha_a^2 k^2(1 + O(\delta_a^2)) \end{aligned} \tag{S47}$$

Of particular interest is the long-wavelength part – with $s = s'$ – of the vertical derivative of $\phi_{a,2,p}$, given by,

$$\begin{aligned} \frac{\partial\phi_{a,2,p}}{\partial z} &\simeq +\sum \mathrm{i}s\frac{g^2}{4\alpha_a^2 k^2}(1 - O(\delta_a^2))\frac{2\sigma(k_a + k'_a)}{\sigma\sigma'}\left(\mathbf{k}\cdot\mathbf{k}' - k_a k'_a\right) Z Z' \mathrm{e}^{-(k_a+k'_a)z}\mathrm{e}^{\mathrm{i}\Theta}, \\ &\simeq +\sum \mathrm{i}s\frac{g^2}{4\alpha_a^2 k^2}(1 - O(\delta_a^2))\frac{2\sigma(k + k')(1 - \delta_a^2)}{\sigma\sigma'}\left(\mathbf{k}\cdot\mathbf{k}' - kk' - 2kk'\delta_a^2\right) Z Z' \mathrm{e}^{-(k_a+k'_a)z}\mathrm{e}^{\mathrm{i}\Theta}, \\ &\simeq +\sum \mathrm{i}s\delta_a^2\frac{g}{\sigma}\left(\mathbf{k}\cdot\mathbf{k}' - kk'\right)(1 + O(\delta_a^2)) Z Z' \mathrm{e}^{-(k_a+k'_a)z}\mathrm{e}^{\mathrm{i}\Theta}, \\ &\simeq -\sum \mathrm{i}s\delta_a^2 2\sigma' k Z Z' \mathrm{e}^{-(k_a+k'_a)z}\mathrm{e}^{\mathrm{i}\Theta}. \end{aligned} \tag{S48}$$

S3.3 The BGKN terms - $F_{j,2}$, $Q_{j,2}$, R_2

S3.3.1 In the water layer

To simplify the calculation of these terms we use $kh \gg 1$ for waves in deep water, and $k_{w0} \simeq k$, we may also use eq. (S27) and eq. (S28). These simplifications lead to :

$$\phi_{w,1} = \sum -\mathrm{i}\frac{s\sigma}{k}\mathrm{e}^{k_{w0}z}\mathrm{e}^{\gamma_w z} Z \mathrm{e}^{\mathrm{i}(\mathbf{k}\cdot\mathbf{x} - s\sigma t)} \tag{S49}$$

And then we obtain the second order terms :

$$\begin{aligned} F_{w,2}(z=0) &= \left.\frac{\mathcal{P}_{w,1}^2}{2\alpha_w^2}\right|_0 - \left.\frac{\left(\nabla\phi_{w,1}\right)^2}{2}\right|_0 \\ &= \sum \frac{ss'\sigma\sigma'}{2kk'}\left[(\frac{s\sigma s'\sigma'}{\alpha_w^2} - \mathbf{k}\mathbf{k}' + kk')\right] ZZ'\mathrm{e}^{\mathrm{i}\Theta} \\ &\simeq \sum \sigma^2\left[1+\delta_a^2(\frac{n^2}{2} - \sin^2\theta_a\left[1-\cos^2(\varphi_2-\varphi)\right]\right] ZZ'\mathrm{e}^{\mathrm{i}\Theta} \end{aligned} \tag{S50}$$

Using the law of cosines in a triangle,

$$k'^2 = k^2 + K^2 - 2\mathbf{k}\cdot\mathbf{K} \tag{S51}$$

so that

$$\sqrt{k'} = \sqrt{k}\left(1+\frac{K^2-2\mathbf{k}\cdot\mathbf{K}}{k^2}\right)^{1/4} \simeq \sqrt{k}\left(1+\frac{1}{4}\frac{K^2-2\mathbf{k}\cdot\mathbf{K}}{k^2}\right) \tag{S52}$$

we get

$$\begin{aligned} Q_{w,2}|_{z=0} &= + \left.\frac{\partial^2\phi_{w,1}}{\partial z^2}\right|_0 \zeta_1 - \nabla\phi_{w,1}|_0\cdot\nabla\zeta_1 \\ &\simeq -\mathrm{i}\sum\left[\frac{s\sigma k + s'\sigma'k'}{2} + \frac{\mathbf{k}\cdot\mathbf{k}'}{2}\left(\frac{s\sigma}{k}+\frac{s'\sigma'}{k'}\right)\right] ZZ'\mathrm{e}^{\mathrm{i}\Theta} \\ &= -\mathrm{i}\sum\left[s\sigma\frac{1}{2k}\left(k^2+\mathbf{k}\cdot\mathbf{k}'\right) + s'\frac{\sigma'}{2k'}\left(k'^2+\mathbf{k}\cdot\mathbf{k}'\right)\right] ZZ'\mathrm{e}^{\mathrm{i}\Theta} \\ &\simeq -\mathrm{i}\sum\left[s\sigma\frac{\mathbf{k}\cdot(\mathbf{k}+\mathbf{k}')}{2k} + s'\sigma'\frac{\mathbf{k}'\cdot(\mathbf{k}'+\mathbf{k})}{2k'}\right] ZZ'\mathrm{e}^{\mathrm{i}\Theta} \\ &\simeq -\mathrm{i}\sum\left[s\sigma\frac{\mathbf{k}\cdot\mathbf{K}}{2k} + s'\sigma'\frac{\mathbf{k}'\cdot\mathbf{K}}{2k'}\right] ZZ'\mathrm{e}^{\mathrm{i}\Theta} \\ &\simeq -\mathrm{i}\sum s\left[\frac{\sigma}{2k}\left(\mathbf{k}\cdot\mathbf{K}+\mathbf{k}'\cdot\mathbf{K}\right) + \frac{\sigma'k-\sigma k'}{2k'k}\left(\mathbf{k}'\cdot\mathbf{K}\right)\right] ZZ'\mathrm{e}^{\mathrm{i}\Theta} \\ &\simeq -\mathrm{i}\sum s\sigma k\left[\frac{K^2}{2k^2} + \sqrt{g}\frac{\sqrt{k}-\sqrt{k'}}{2k\sigma\sqrt{kk'}}\left(-\mathbf{k}\cdot\mathbf{K}+K^2\right)\right] ZZ'\mathrm{e}^{\mathrm{i}\Theta} \\ &\simeq -\mathrm{i}\sum s\sigma k\left[2\delta_a^2\sin^2\theta_a + \frac{1}{4k^2}\left(2\mathbf{k}\cdot\mathbf{K}-K^2\right)\right)\frac{1}{2k^2}\left(-\mathbf{k}\cdot\mathbf{K}+K^2\right)\right] ZZ'\mathrm{e}^{\mathrm{i}\Theta} \\ &\simeq -\mathrm{i}\sum s\sigma k\left[2\delta_a^2\sin^2\theta_a - \frac{K^2}{4k^2}\left(\frac{\mathbf{k}\cdot\mathbf{K}}{kK}\right)^2\right] ZZ'\mathrm{e}^{\mathrm{i}\Theta} \\ &\simeq -\mathrm{i}\sum s\sigma k\left[2\delta_a^2\sin^2\theta_a\left(1-\frac{1}{2}\cos^2(\varphi_2-\varphi)\right)\right] ZZ'\mathrm{e}^{\mathrm{i}\Theta}. \end{aligned} \tag{S53}$$

S3.3.2 In the air

In a similar way we obtain :

Then,

$$
\begin{aligned}
F_{a,2}(z=0) &= \left.\frac{\mathcal{P}_{w,1}^2}{2\alpha_w^2}\right|_0 - \left.\frac{\left(\nabla\phi_{w,1}\right)^2}{2}\right|_0 \\
&= \sum \frac{ss'\sigma\sigma'}{2k_a k'_a}\left[\frac{s\sigma s'\sigma'}{\alpha_a^2} - \mathbf{k}\mathbf{k}' + k_a k'_a\right] ZZ' \mathrm{e}^{\mathrm{i}\Theta} \\
&= \sum ss'\sigma\sigma'(1+2\delta_a^2)\left[\frac{s\sigma s'\sigma'}{2kk'\alpha_a^2} - \frac{\mathbf{k}\mathbf{k}' - kk' + 2\delta_a^2 kk'}{2kk'}\right] ZZ' \mathrm{e}^{\mathrm{i}\Theta} \\
&\simeq \sum \sigma^2\left[1+\delta_a^2\left(\frac{3}{2} - \sin^2\theta_a\left[1-\cos^2(\varphi_2-\varphi)\right]\right)\right] ZZ' \mathrm{e}^{\mathrm{i}\Theta} \qquad \text{(S54)}
\end{aligned}
$$

And using :

$$
\begin{aligned}
\frac{s\sigma k + s'\sigma' k'}{2} - \frac{\mathbf{k}\cdot\mathbf{k}'}{2}\left(\frac{s\sigma}{k} + \frac{s'\sigma'}{k'}\right) &= s\sigma\frac{1}{2k}\left(k^2 - \mathbf{k}\cdot\mathbf{k}'\right) + s'\frac{\sigma'}{2k'}\left(k'^2 - \mathbf{k}\cdot\mathbf{k}'\right) \\
&= s\sigma\frac{1}{2k}\left(2k^2 - \mathbf{k}\cdot\mathbf{K}\right) + s'\frac{\sigma'}{2k'}\left(2k'^2 - \mathbf{k}'\cdot\mathbf{K}\right) \\
&= s\sigma k + s'\sigma' k' - \left[s\sigma\frac{\mathbf{k}\cdot\mathbf{K}}{2k} + s'\sigma'\frac{\mathbf{k}'\cdot\mathbf{K}}{2k'}\right] \\
&\simeq s\sigma k\left[2 - 2\delta_a^2\sin^2\theta_a\left(1 - \frac{1}{2}\cos^2(\varphi_2-\varphi)\right)\right] \qquad \text{(S55)}
\end{aligned}
$$

one gets :

$$
\begin{aligned}
Q_{a,2}|_{z=0} &= +\left.\frac{\partial^2\phi_{a,1}}{\partial z^2}\right|_0 \zeta_1 - \nabla\phi_{a,1}|_0 \cdot \nabla\zeta_1 \\
&= +\mathrm{i}\sum\left[\frac{s\sigma k_a + s'\sigma' k'_a}{2} + \frac{\mathbf{k}\cdot\mathbf{k}'}{2}\left(\frac{s\sigma}{k_a} + \frac{s'\sigma'}{k'_a}\right)\right] ZZ' \mathrm{e}^{\mathrm{i}\Theta} \\
&= +\mathrm{i}\sum\left[\frac{s\sigma k + s'\sigma' k'}{2}(1-\delta_a^2) + \frac{\mathbf{k}\cdot\mathbf{k}'}{2}\left(\frac{s\sigma}{k} + \frac{s'\sigma'}{k'}\right)(1+\delta_a^2)\right] ZZ' \mathrm{e}^{\mathrm{i}\Theta} \\
&= +\mathrm{i}\sum\left[\frac{s\sigma k + s'\sigma' k'}{2} + \frac{\mathbf{k}\cdot\mathbf{k}'}{2}\left(\frac{s\sigma}{k} + \frac{s'\sigma'}{k'}\right) - \delta_a^2\cdot\left(\frac{s\sigma k + s'\sigma' k'}{2} - \frac{\mathbf{k}\cdot\mathbf{k}'}{2}\left(\frac{s\sigma}{k} + \frac{s'\sigma'}{k'}\right)\right)\right] ZZ' \mathrm{e}^{\mathrm{i}\Theta} \\
&\simeq +\mathrm{i}\sum s\sigma k 2\delta_a^2\left[\sin^2\theta_a\left(1 - \frac{1}{2}\cos^2(\varphi_2-\varphi)\right) - \left[1 - \delta_a^2\sin^2\theta_a\left(1 - \frac{1}{2}\cos^2(\varphi_2-\varphi)\right)\right]\right] ZZ' \mathrm{e}^{\mathrm{i}\Theta} \\
&\simeq -\mathrm{i}\sum s\sigma k 2\delta_a^2\left[1 - \sin^2\theta_a\left(1 - \frac{1}{2}\cos^2(\varphi_2-\varphi)\right)(1+\delta_a^2)\right] ZZ' \mathrm{e}^{\mathrm{i}\Theta} \qquad \text{(S56)}
\end{aligned}
$$

S3.3.3 R_2 coefficient

$$
\begin{aligned}
R_2 = & -\left(\frac{\partial \mathcal{P}_{w,1}}{\partial z} - m\frac{\partial \mathcal{P}_{a,1}}{\partial z}\right)_0 \zeta_1 + \frac{g}{\alpha_a^2}(n^2\mathcal{P}_{w,1} - m\mathcal{P}_{a,1})_0\zeta_1 - \frac{g^2}{2\alpha_a^2}(n^2-m^2)\zeta_1^2 \\
= & \sum\left[\frac{\sigma^2+\sigma'^2}{2}\cdot(1-m) - \delta_a^2\frac{\sigma^2+\sigma'^2}{2}(n^2+m(1+\delta_a^2)) - \frac{\delta_a^2}{2}\frac{\sigma^2+\sigma'^2}{2}(n^2-m^2)\right] ZZ'\mathrm{e}^{\mathrm{i}\Theta} \\
\simeq & \sum\left[\sigma^2\cdot\left(1-m-\delta_a^2\left(\frac{3n^2}{2}+m\left(1-\frac{m}{2}+\delta_a^2\right)\right)\right)\right] ZZ'\mathrm{e}^{\mathrm{i}\Theta} \qquad \text{(S57)}
\end{aligned}
$$

S4 MATRIX PROBLEM FOR THE SECOND ORDER AMPLITUDES

• Velocity continuity at $z = 0$

$$\left.\frac{\partial \phi_{a,2}}{\partial z}\right|_0 + Q_{a,2} = \left.\frac{\partial \phi_{w,2}}{\partial z}\right|_0 + Q_{w,2} \tag{S58}$$

$$\iff \nu_+ A_+ - \mu_- W_- - \mu_+ W_+ = \left.\frac{\partial \Phi_{w,2,p}}{\partial z}\right|_0 - \left.\frac{\partial \Phi_{a,2,p}}{\partial z}\right|_0 - Q_{a,2} + Q_{w,2} \tag{S59}$$

• Pressure continuity at $z = 0$

$$\left(\frac{\partial \mathcal{P}_{w,2}}{\partial t} - m\frac{\partial \mathcal{P}_{a,2}}{\partial t}\right)_0 - g(1-m)\frac{\partial \zeta_2}{\partial t} = \frac{\partial R_2}{\partial t}$$

$$\iff \left(\frac{\partial \mathcal{P}_{w,2}}{\partial t} - m\frac{\partial \mathcal{P}_{a,2}}{\partial t}\right)_0 - g(1-m)\left.\frac{\partial \phi_{a,2}}{\partial z}\right|_0 - g(1-m)Q_{a,2} = \frac{\partial R_2}{\partial t}$$

$$\iff -\left.\frac{\partial^2 \phi_{w,2}}{\partial t^2}\right|_0 + \left.\frac{\partial F_{w,2}}{\partial t}\right|_0 + m\left.\frac{\partial^2 \phi_{a,2}}{\partial t^2}\right|_0 - m\left.\frac{\partial F_{a,2}}{\partial t}\right|_0 - g(1-m)\left.\frac{\partial \phi_{a,2}}{\partial z}\right|_0 - g(1-m)Q_{a,2} = \frac{\partial R_2}{\partial t}$$

$$\iff -\Omega^2\left(-\phi_{w,2,p}(0) - W_+ - W_- + m\phi_{a,2,p}(0) + mA_+\right) + \mathrm{i}\Omega(mF_{a,2}(0) - F_{w,2}(0))$$

$$-g(1-m)(\phi'_{a,2,p}(0) + \nu A_+ + Q_{a,2}) = \frac{\partial R_2}{\partial t} \tag{S60}$$

• Boundary condition at $z = -h$

This boundary condition is given as an example, a more realistic boundary condition will be developed further:

$$\frac{\partial \Phi_{w,2,p}}{\partial z}(-h) + \mu_- W_- \mathrm{e}^{-\mu_- h} + \mu_+ W_2 \mathrm{e}^{-\mu_+ h} = 0 \tag{S61}$$

Then we can write the boundary conditions system as a matrix problem,

$$\begin{pmatrix} \nu & -\mu_- & -\mu_+ \\ -m\Omega^2 - g(1-m)\nu & \Omega^2 & \Omega^2 \\ 0 & \mu_- \mathrm{e}^{-\mu_- h} & \mu_+ \mathrm{e}^{-\mu_+ h} \end{pmatrix} \cdot \begin{pmatrix} A_+ \\ W_- \\ W_+ \end{pmatrix} = \begin{pmatrix} \Lambda_1 \\ \Lambda_2 \\ \Lambda_3 \end{pmatrix} \tag{S62}$$

Because we have assumed $kh \gg 1$ we can neglect the p_{bot} term of (Ardhuin & Herbers, 2013) in Λ_3, and the Λ forcing terms are,

$$\Lambda_1 = \left.\frac{\partial \phi_{w,2,p}}{\partial z}\right|_0 - \left.\frac{\partial \phi_{a,2,p}}{\partial z}\right|_0 - Q_{a,2} + Q_{w,2} \tag{S63}$$

$$\Lambda_2 = -\Omega^2\left(\phi_{w,2,p}(0) - m\phi_{a,2,p}(0)\right) - \mathrm{i}\Omega\left(mF_{a,2}(0) - F_{w,2}(0)\right) + g(1-m)(\phi'_{a,2,p}(0) + Q_{a,2}) + \frac{\partial R_2}{\partial t}$$

$$\Lambda_3 = -\left.\frac{\partial \phi_{w,2,p}}{\partial z}\right|_{-h} \tag{S64}$$

SIMPLIFIED FORMS USED:

$$F_{w,2}(z=0) \simeq \sum \sigma^2[1-\sin^2\theta_a\delta_a^2(1-\cos^2(\varphi_2-\varphi)) + \frac{\delta_a^2 n^2}{2}]ZZ'\mathrm{e}^{i\Theta} \quad \mathbf{O(\sigma^2) + O(\sigma^2\delta_a^2\sin^2\theta_a)}$$

$$Q_{w,2}(z=0) \simeq -\mathrm{i}\sum s\sigma k2\sin^2\theta_a\delta_a^2(1-\frac{1}{2}\cos^2(\varphi_2-\varphi))ZZ'\mathrm{e}^{i\Theta} \quad \mathbf{O(\sigma\delta_a^2\sin^2\theta_a)}$$

$$F_{a,2}(z=0) \simeq \sum \sigma^2[1-\sin^2\theta_a\delta_a^2(1-\cos^2(\varphi_2-\varphi)) + \frac{3}{2}\delta_a^2]ZZ'\mathrm{e}^{i\Theta} \quad \mathbf{O(\sigma^2) + O(\sigma^2\delta_a^2\sin^2\theta_a)}$$

$$Q_{a,2}(z=0) \simeq -\mathrm{i}\sum s\sigma k2\delta_a^2[1-\sin^2\theta_a(1-\frac{1}{2}\cos^2(\varphi_2-\varphi))]ZZ'\mathrm{e}^{i\Theta} \quad \mathbf{O(\sigma\delta_a^2) + O(\sigma\delta_a^2\sin^2\theta_a)}$$

$$\phi_{w,2,p}(z=0) \simeq \mathrm{i}\sum s\sigma\delta_a^2 n^2 ZZ'\mathrm{e}^{i\Theta} \quad \mathbf{O(\sigma\delta_a^2 n^2)}$$

$$\left.\frac{\partial\phi_{w,2,p}}{\partial z}\right|_{z=0} \simeq \mathrm{i}\sum s\sigma 2k\delta_a^2 n^2 ZZ'\mathrm{e}^{i\Theta} \quad \mathbf{O(\sigma\delta_a^2 n^2)}$$

$$\phi_{a,2,p}(z=0) \simeq \mathrm{i}\sum s\sigma\delta_a^2 ZZ'\mathrm{e}^{i\Theta} \quad \mathbf{O(\sigma\delta_a^2) + O(\sigma\delta_a^2\sin^2\theta_a)}$$

$$\left.\frac{\partial\phi_{a,2,p}}{\partial z}\right|_{z=0} \simeq -\mathrm{i}\sum s\sigma 2k\delta_a^2 ZZ'\mathrm{e}^{i\Theta} \quad \mathbf{O(\sigma\delta_a^2)}$$

$$R_2 \simeq \sum -\sigma^2(1-m-\delta_a^2(3n^2/2+m))ZZ'\mathrm{e}^{i\Theta} \quad \mathbf{O(\sigma^2)}$$

$$\frac{\partial R_2}{\partial t} \simeq \mathrm{i}s\sum 2\sigma^3(1-m-\delta_a^2(3n^2/2+m))ZZ'\mathrm{e}^{i\Theta} \quad \mathbf{O(\sigma^3)}$$

$$\nu_\pm = 2\mathrm{i}\delta_a k(\pm\cos\theta_a - \mathrm{i}\frac{\delta_a}{4})$$

$$\mu_\pm = 2\mathrm{i}\delta_a k(\mp\mathrm{i}l - \mathrm{i}\frac{\delta_a}{4}n^2)$$

$$\sin\theta_a = \frac{K\alpha_a}{\Omega},$$

$$\Omega \simeq 2\sigma, \qquad n = \frac{\alpha_a}{\alpha_w}, \qquad l = (\sin^2\theta_a - n^2)^{1/2},$$

$$\delta_w = \left(\frac{g}{k\alpha_a^2}\right)^{1/2}\frac{\alpha_a}{\alpha_w} = \delta_a n$$

S4.1 Matrix 2x2 : BGKN73

When the ocean is assumed to have an infinite depth, we consider the atmosphere and ocean to be half spaces, with the continuity of velocity and pressure at $z = 0$ giving a 2 by 2 matrix,

$$M = \begin{pmatrix} \nu & -\mu_- \\ -m\Omega^2 - g(1-m)\nu & \Omega^2 \end{pmatrix} \tag{S65}$$

The solution is given by Cramer's method

$$A_+ = \frac{\det \mathbf{M}_1}{\det \mathbf{M}} \tag{S66}$$

with

$$\det \mathbf{M}_1 = \begin{vmatrix} \Lambda_1 & -\mu_- \\ \Lambda_2 & \Omega^2 \end{vmatrix} \tag{S67}$$

$$\det \mathbf{M} = \begin{vmatrix} \nu & -\mu_- \\ -m\Omega^2 - g(1-m)\nu & \Omega^2 \end{vmatrix} = \nu\Omega^2 - m\mu_-\Omega^2 - g(1-m)\nu\mu_- \tag{S68}$$

Here are the different pieces of $\det \mathbf{M}$,

- $\nu\Omega^2$:

$$\begin{aligned} \nu\Omega^2 &= 4\sigma^2 \left(\frac{g}{2\alpha_a^2} + \mathrm{i}\frac{\Omega}{\alpha_a}\cos\theta_a \right) \\ &= \mathrm{i}8\sigma^2 k \left(-\mathrm{i}\frac{g}{4k\alpha^2} + \frac{\sigma}{k\alpha_a}\cos\theta_a \right) \\ &= 8\mathrm{i}\sigma^2 k\delta_a \left(\cos\theta_a - \mathrm{i}\frac{\delta_a}{4} \right) \end{aligned}$$

- $-m\mu_-\Omega^2$:

$$\begin{aligned} -m\mu_-\Omega^2 &\simeq -m4\sigma^2 \cdot 2\mathrm{i}\delta_a k \left[\mathrm{i}l - \mathrm{i}\frac{\delta_a}{2}n^2 \right] \\ &\simeq -8\mathrm{i}\sigma^2 k\delta_a m \left[\mathrm{i}l \right] \end{aligned}$$

- $-g(1-m)\nu\mu_-$,

$$\begin{aligned} -g(1-m)\nu\mu_- &\simeq -g(1-m)2\mathrm{i}\delta_a k \left(\cos\theta_a - \mathrm{i}\frac{\delta_a}{4} \right) 2\mathrm{i}\delta_a k \left(\mathrm{i}l + \mathrm{i}\frac{\delta_a}{4}n^2 \right) \\ &\simeq 4\sigma^2\delta_a k\delta_a(\mathrm{i}l\cos\theta_a + O(\delta_a)) \\ &\simeq 8\mathrm{i}\sigma^2 k\delta_a \left[\frac{1}{2}\delta_a l\cos\theta_a \right] \end{aligned}$$

This gives $\det \mathbf{M}$, keeping only δ_a^2 (one is in factor and should be remove when doing the ratio),

$$\begin{aligned} \det \mathbf{M} &= \mathrm{i}8\sigma^2\delta_a k \left[-\mathrm{i}\frac{\delta_a}{4} + \cos\theta_a - \mathrm{i}ml + \frac{\delta_a}{2}\cos\theta_a l \right] \\ \det \mathbf{M} &\simeq 8\mathrm{i}\sigma^2 k\delta_a \left[\cos\theta_a \left(1 + \frac{\delta_a}{2}l \right) - \mathrm{i}\left(\frac{\delta_a}{4} + ml \right) \right] \end{aligned} \tag{S69}$$

In *green* there is a difference with BGKN73 denominator, that is coming from the $\partial\zeta_2/\partial t$ term in the Bernoulli equation for the pressure at $z = 0$.

Now the numerator is,

$$\begin{aligned}
\det \mathbf{M}_1 &= \Lambda_1\Omega^2 + \mu_-\Lambda_2 \\
&= \Omega^2\left(\left.\frac{\partial\phi_{w,2,p}}{\partial z}\right|_0 - \left.\frac{\partial\phi_{a,2,p}}{\partial z}\right|_0 - Q_{a,2} + Q_{w,2}\right) + \mu_-\Bigg(-\Omega^2\big(\Phi_{w,2,p}(0) \\
&\quad -m\Phi_{a,2,p}(0)\big) - \mathrm{i}s\Omega\big(mF_{a,2}(0) - F_{w,2}(0)\big) + g(1-m)(\Phi'_{a,2,p}(0) + Q_{a,2}) + \frac{\partial R_2}{\partial t}\Bigg) \\
&\simeq \Omega^2\left(\left.\frac{\partial\phi_{w,2,p}}{\partial z}\right|_0 - \left.\frac{\partial\phi_{a,2,p}}{\partial z}\right|_0 - Q_{a,2} + Q_{w,2}\right) \\
&\quad + \mu_-\left(\mathrm{i}s\Omega F_{w,2}(0) + \frac{\partial R_2}{\partial t}\right) \qquad \text{(S70)}
\end{aligned}$$

where eqs. (S40), (S48) , (S56), (S50) give

$$\begin{aligned}
\Omega^2\left.\frac{\partial\phi_{w,2,p}}{\partial z}\right|_0 &= 4\sigma^2\cdot \mathrm{i}s\delta_a^2 n^2\sigma 2k \\
&\simeq 8\mathrm{i}\sigma^2 k\delta_a s\sigma\delta_a n^2 \qquad \text{(S71)} \\
-\Omega^2\left.\frac{\partial\phi_{a,2,p}}{\partial z}\right|_0 &= -4\sigma^2\cdot(-\mathrm{i})s2\sigma k\delta_a^2 \\
&\simeq 8\mathrm{i}\sigma^2 k\delta_a s\sigma\delta_a \qquad \text{(S72)} \\
-\Omega^2 Q_{a,2} &\simeq -4\sigma^2\cdot(-\mathrm{i})s2\sigma k\delta_a^2\left(1-\sin^2\theta_a\left(1-\frac{1}{2}\cos^2(\varphi_2-\varphi)\right)\right) \\
&\simeq 8\mathrm{i}\sigma^2 k\delta_a\sigma s\delta_a\left(1-\sin^2\theta_a\left(1-\frac{1}{2}\cos^2(\varphi_2-\varphi)\right)\right) \qquad \text{(S73)} \\
+\Omega^2 Q_{w,2} &\simeq 4\sigma^2\cdot \mathrm{i}2\sigma s k\delta_a^2\left(-\sin^2\theta_a\left(1-\frac{1}{2}\cos^2(\varphi_2-\varphi)\right)\right) \\
&\simeq 8\mathrm{i}\sigma^2 k\delta_a\sigma s\delta_a\left(-\sin^2\theta_a\left(1-\frac{1}{2}\cos^2(\varphi_2-\varphi)\right)\right) \qquad \text{(S74)} \\
+\mathrm{i}s\Omega\mu_- F_{w,2}(0) &\simeq \mathrm{i}2s\sigma\cdot 2\delta_a k(\frac{\delta_a}{4}n^2 - l)\cdot\sigma^2[1-\sin^2\theta_a\delta_a^2(1-\cos^2(\varphi_2-\varphi)) + \delta_a^2 n^2/2] \\
&\simeq -8\mathrm{i}\sigma^2 k\delta_a\sigma s\left[\frac{l}{2} - \frac{\delta_a}{8}n^2 - \frac{l}{2}\sin^2\theta_a\delta_a^2\left[1-\cos^2(\varphi_2-\varphi)\right]\right] \qquad \text{(S75)} \\
\mu_-\frac{\partial R_2}{\partial t} &= 2\delta_a k\left(\frac{\delta_a}{4}n^2 - l\right)\mathrm{i}s2\sigma^3(1-m) \\
&\simeq -8\mathrm{i}\delta_a k\sigma^2\sigma s\left[\frac{l}{2} - \frac{\delta_a}{8}n^2\right]
\end{aligned}$$

Collecting all the terms we find,

$$\det \mathbf{M}_1 \simeq -8\mathrm{i}\sigma^2 k\delta_a \sigma s \left[l - \frac{\delta_a}{4} n^2 - \delta_a + 2\delta_a \sin^2\theta_a (1 - \frac{1}{2}\cos^2\varphi_2) + \delta_a \left(n^2 - 1\right) \right]$$
$$\simeq -8\mathrm{i}\sigma^2 k\delta_a \sigma s \left[l - \delta_a \left[2 - 2\sin^2\theta_a (1 - \frac{1}{2}\cos^2\varphi_2) + \frac{5}{4} n^2 \right] \right]$$
$$\simeq -8\mathrm{i}\sigma^2 k\delta_a \sigma s \left[l - 2\delta_a \left[1 - \sin^2\theta_a (1 - \frac{1}{2}\cos^2\varphi_2) + \frac{5}{8} n^2 \right] \right] \tag{S76}$$

Then, we find the same expression as in BGKN73 numerator and the δ_a term is larger than the one in WG06, with 2 instead of 3/2.

The main term arises from the pressure boundary condition and from the difference between the pressure and the temporal derivative of the potential velocity.

We recall that the homogeneous atmospheric potential that radiates from the surface is given by eq. (S41),

$$\phi_{a,h,2}(z) = \sum s A_+ Z Z' \mathrm{e}^{\nu+z} \mathrm{e}^{\mathrm{i}\Theta}, \tag{S77}$$

with

$$\nu \simeq \frac{g}{2\alpha_a^2} + \mathrm{i}\frac{\Omega}{\alpha_a}\cos\theta_a \tag{S78}$$

and

$$A_+ \simeq -\sigma \frac{l - 2\delta_a \left[1 - \sin^2\theta_a \left(1 - \frac{1}{2}\cos^2(\varphi_2 - \varphi)\right) + \frac{5}{8}n^2\right]}{\cos\theta_a \left(1 + \frac{\delta_a}{2} l\right) - \mathrm{i}\left(\frac{\delta_a}{4} + ml\right)}. \tag{S79}$$

S5 ADDING THE SOLID EARTH

The solid Earth is characterized by density ρ_s, compression velocity α_s and shear velocity β.

Then the velocity potential writes,

$$\phi_{w,2} = \sum \left[\left(W_- \mathrm{e}^{\mu - z} + W_+ \mathrm{e}^{\mu + z} \right) Z Z' + \Phi_{w,2,p} \right] \mathrm{e}^{\mathrm{i}\Theta}, \qquad \text{for } -h < z < \zeta \tag{S80}$$

$$\phi_{a,2} = \sum \left[s A_+ \mathrm{e}^{\nu+z} Z Z' + \Phi_{w,2,p} \right] \mathrm{e}^{\mathrm{i}\Theta}, \qquad \text{for } \zeta < z \tag{S81}$$

All the potentials share the same phase, $\Theta = \mathbf{K}\cdot\mathbf{x} - \Omega t$, $\Omega = s(\sigma + \sigma')$, but they differ by their vertical structures and amplitudes.

The boundary conditions for ocean/atmosphere interfaces remain the same. For the ocean bottom, the motion in the crust is given by velocity potentials for compression and shear waves in the

solid Earth, we follow here the treatment in (Ardhuin & Herbers, 2013). Neglecting the effect of gravity, crustal motions can be separated in an irrotational part with a velocity potential ϕ_c and a rotational part with a stream function ψ, both solutions to Laplace's equation.

$$\phi_c = C_p \mathrm{e}^{\chi_p (z+h)} \mathrm{e}^{\mathrm{i}\Theta}, \tag{S82}$$

$$\psi = C_s \mathrm{e}^{\chi_s (z+h)} \mathrm{e}^{\mathrm{i}\Theta}, \tag{S83}$$

with

$$\chi_p = \sqrt{K^2 - \frac{\Omega^2}{\alpha_s^2}}, \quad \text{and} \quad \chi_s = \sqrt{K^2 - \frac{\Omega^2}{\beta^2}}. \tag{S84}$$

where α_s and β are respectively the compression and the shear wave speed in crust. Typically β ranges from 2800 to 3200 m s^{-1}; and $\alpha_s = \sqrt{3}\beta$. And $\rho_s \simeq 2500$ kg m^{-3}. The constants C_p and C_s have dimensions of m^2/s and are determined by the boundary conditions at the ocean bottom.

With λ_e and μ_e the Lame elasticity parameters of the crust, Hooke's law of elasticity gives

$$\tau_{zz} = \lambda_e \left(\frac{\partial \xi_x}{\partial x} + \frac{\partial \xi_z}{\partial z} \right) + 2\mu_e \frac{\partial \xi_z}{\partial z}, \tag{S85}$$

$$\tau_{xz} = \mu_e \left(\frac{\partial \xi_x}{\partial z} + \frac{\partial \xi_z}{\partial x} \right). \tag{S86}$$

We recall that the compression and shear velocity are related to the Lame parameters,

$$\alpha_c^2 = \frac{\lambda_e + 2\mu_e}{\rho_s}, \tag{S87}$$

$$\beta^2 = \frac{\mu_e}{\rho_s}. \tag{S88}$$

The zero tangential stress on the ocean bottom $\tau_{xz}(z = -h) = 0$ yields the following relationship between C_p and C_s, which is typical of seismic Rayleigh waves (Stoneley, 1926),

$$C_s = \frac{2\mathrm{i}K\chi_p}{\chi_s^2 + K^2} C_p = \frac{2\mathrm{i}\beta^2 K \chi_p}{2\beta^2 K^2 - \Omega^2} C_p. \tag{S89}$$

We can now eliminate also C_p using the continuity of the vertical velocity at the bottom,

$$\frac{\partial \phi_2}{\partial z} = \frac{\partial \phi_c}{\partial z} + \frac{\partial \psi}{\partial x} \quad \text{at} \quad z = -h \tag{S90}$$

$$W_+ \mu_+ \mathrm{e}^{-\mu_+ h} + W_- \mu_- \mathrm{e}^{-\mu_- h} = \chi_p C_p + \mathrm{i}K C_s \tag{S91}$$

$$= \chi_p C_p + \mathrm{i}K \frac{2\mathrm{i}\beta^2 K \chi_p}{2\beta^2 K^2 - \Omega^2} C_p \tag{S92}$$

$$= \frac{\chi_p \Omega^2}{\Omega^2 - 2K^2\beta^2} C_p \tag{S93}$$

and the continuity of normal stresses, using the result from (Ardhuin et al., 2013) is

$$-\rho_w \frac{\partial \phi_2}{\partial t} = \tau_{zz} \quad z = -h \tag{S94}$$

$$\rho_w \Omega \mathrm{i} s \mathrm{e}^{-\mu_+ h} W_+ + \rho_w \Omega \mathrm{i} s W_- \mathrm{e}^{-\mu_- h} = r_{AH} C_p \tag{S95}$$

$$\tag{S96}$$

where

$$r_{AH} = \frac{\mathrm{i}s}{\Omega} \rho_s \left[-\frac{4\beta^4 K^2 \chi_p \chi_s}{\Omega^2 - 2K^2\beta^2} + \left(\Omega^2 - 2K^2\beta^2\right) \right]. \tag{S97}$$

Defining

$$r_\pm = \frac{\mathrm{i}s\rho_w \Omega \dfrac{\chi_p \Omega^2}{\Omega^2 - 2K^2\beta^2}}{\mu_\pm r_{AH}} \tag{S98}$$

$$= \frac{\mathrm{i}s\rho_w \Omega \dfrac{\chi_p \Omega^2}{\Omega^2 - 2K^2}}{\dfrac{\mathrm{i}}{\Omega} \mu_\pm \rho_s \left[-\dfrac{4\beta^4 K^2 \chi_p \chi_s}{\Omega^2 - 2K^2\beta^2} + \left(\Omega^2 - 2K^2\beta^2\right) \right]}, \tag{S99}$$

$$= \frac{\rho_w \chi_p \Omega^4}{\mu_\pm \rho_s \left[\left(\Omega^2 - 2K^2\beta^2\right)^2 - 4\beta^4 K^2 \chi_p \chi_s \right]} \tag{S100}$$

we combine these two boundary conditions by subtracting r times the second equation to find a condition for the bottom velocities on the water side,

$$\mu^+ (1 - r_+) \mathrm{e}^{-\mu_+ h} W_+ + \mu^- (1 - r_-) \mu_- \mathrm{e}^{-\mu_- h} W_- = 0. \tag{S101}$$

We thus have the matrix equation

$$\mathbf{M}(A_+,\ W_-,\ W_+)^T = (\Lambda_1,\ \Lambda_2,\ 0)^T \tag{S102}$$

with

$$\mathbf{M} = \begin{pmatrix} \nu_+ & -\mu_- & -\mu_+ \\ -m\Omega^2 - g(1-m)\nu_+ & \Omega^2 & \Omega^2 \\ 0 & (1 - r_-)\,\mu_- \mathrm{e}^{-\mu_- h} & (1 - r_+)\,\mu_+ \mathrm{e}^{-\mu_+ h} \end{pmatrix} \tag{S103}$$

and we use the following simplification,

$$\Lambda_1 = \left. \frac{\partial \Phi_{w,2,p}}{\partial z} \right|_0 - \left. \frac{\partial \Phi_{a,2,p}}{\partial z} \right|_0 - Q_{a,2} + Q_{w,2} \tag{S104}$$

$$\Lambda_2 = \mathrm{i}\Omega F_{w,2}(0) + \frac{\partial R_2}{\partial t} \tag{S105}$$

380 Assuming $mu_+ \simeq -\mu_- \simeq \mu$ the matrix equation simplifies as:

381
$$\mathbf{M} = \begin{pmatrix} \nu_+ & \mu & -\mu \\ -m\Omega^2 - g(1-m)\nu_+ & \Omega^2 & \Omega^2 \\ 0 & -(1+r)\,\mu \mathrm{e}^{\mu h} & (1-r)\,\mu \mathrm{e}^{-\mu h} \end{pmatrix} \tag{S106}$$

S6 FROM AMPLITUDE TO POWER

S6.1 Particular case of a pair of wave trains

Here we first consider the pressure amplitude and variance in the water layer, which has been well studied and measured (Cox & Jacobs, 1989; Ardhuin et al., 2013).

In the case of only two wave trains of opposing direction with wave numbers k_1 and $k_2 \simeq -k_1$ with surface elevation

$$\zeta = a_1 \cos(k_1 x - \sigma_1 t) + a_2 \cos(k_2 x - \sigma_2 t) \tag{S107}$$

and velocity field

$$w(z=0) = a_1\sigma_1 \sin(k_1 x - \sigma_1 t) + a_2\sigma_2 \sin(k_2 x - \sigma_2 t) \tag{S108}$$

$$u(z=0) = a_1\sigma_1 \cos(k_1 x - \sigma_1 t) - a_2\sigma_2 \cos(k_2 x - \sigma_2 t) \tag{S109}$$

the second order pressure is, keeping only the small wavenumber components,

$$p_2 = \rho_w(u^2 + w^2) = -2\rho\sigma_1\sigma_2 a_1 a_2 \cos\left[Kx + \Omega t\right] \tag{S110}$$

Now we consider the variance of the pressure,

$$< p_2^2 > = 4\rho_w^2\sigma_1^2\sigma_2^2 a_1^2 a_2^2/2 \tag{S111}$$

$$= 2\rho_w^2 \sum_{k+k'=K} \sigma^2\sigma'^2 a^2 a'^2/2 \tag{S112}$$

$$= 8\rho_w^2\sigma_1^2\sigma_2^2 \frac{a_1^2}{2}\frac{a_2^2}{2} \tag{S113}$$

$$\simeq \frac{1}{2}\rho_w^2\Omega^4 E_1 E_2 \tag{S114}$$

$$= \frac{1}{4}\rho_w^2\Omega^4 \sum_{k+k'=K} EE'. \tag{S115}$$

S6.2 Case of random waves

$$F_{p,2h}(\mathbf{K}, f_s) = 2 \lim_{|d\mathbf{K}|\to 0, df_s \to 0} \frac{\left\langle \left| P_{2h}^{+} \right|^2 \right\rangle}{dK_x dK_y df_s} \tag{S116}$$

with

$$P_{2h}^{s} = \rho_a \mathcal{P}_{a,2,h} = -\rho_a \frac{\partial \phi_{a,2,h}}{\partial t}$$
$$= -\rho_a \frac{\partial}{\partial t}\left(\frac{R_a(\mathbf{K})}{\rho_w 2\sigma'} p_{\text{surf}}^{s,s'}(\mathbf{K},\Omega)\right)$$

remembering

$$p_{\text{surf}}^{s,s'}(\mathbf{K},\Omega) = \rho_w \sum_{\mathbf{k},s,\mathbf{k}',s'} D_z(\mathbf{k},s,\mathbf{k}',s') Z Z' \mathrm{e}^{\mathrm{i}\Theta} \tag{S117}$$

one gets :

$$P_{2h}^{s} = \rho_a \sum_{\mathbf{k},s,\mathbf{k}',s'} \mathrm{i} R_a(\mathbf{K}) \frac{(s\sigma + s'\sigma')}{2\sigma'} D_z(\mathbf{k},s,\mathbf{k}',s') Z Z' \mathrm{e}^{\mathrm{i}\Theta}$$
$$= \rho_a \sum_{\mathbf{k},s,\mathbf{k}'} \mathrm{i} s R_a(\mathbf{K}) \frac{(\sigma + \sigma')}{2\sigma'} D_z(\mathbf{k},s,\mathbf{k}',s) Z Z' \mathrm{e}^{\mathrm{i}\Theta} \tag{S118}$$

Then,

$$2|P_{2h}^{+}|^2 = 2\rho_a^2 \left| \sum_{\mathbf{k}+\mathbf{k}'=\mathbf{K},\sigma+\sigma'=\Omega} R_a(\mathbf{K}) \frac{(\sigma+\sigma')}{2\sigma'} D_z(\mathbf{k},+,\mathbf{k}',+) Z Z' \mathrm{e}^{\mathrm{i}\Theta} \right|^2$$
$$= 2\rho_a^2 \cdot 2 \sum_{\mathbf{k}+\mathbf{k}'=\mathbf{K},\sigma+\sigma'=\Omega} |R_a(\mathbf{K})|^2 \frac{(\sigma+\sigma')^2}{4\sigma'^2} |D_z(\mathbf{k},+,\mathbf{k}',+)|^2 |Z|^2 |Z'|^2 \tag{S119}$$

And the spectrum density of the source writes :

$$F_{p,2h}(\mathbf{K},f_s) = \lim_{|d\mathbf{K}|\to 0, df_s \to 0} \frac{1}{K_x dK_y df_s} \sum_{\mathbf{k}+\mathbf{k}'=\mathbf{K},\sigma+\sigma'=\Omega} \frac{(\sigma+\sigma')^2}{\sigma'^2} R_a(\mathbf{K})^2 \rho_a^2 |D_z(\mathbf{k},+,\mathbf{k}',+)|^2 |Z|^2 |Z'|^2 \tag{S120}$$

using the definition :

$$E(k_x,k_y) = 2 \lim_{dk_x,dk_y \to 0} \frac{|Z|^2}{dk_x dk_y} \tag{S121}$$

$$F_{p,2h}(\mathbf{K},f_s) = \lim_{|d\mathbf{K}|\to 0, df_s \to 0} \frac{dk_x dk_x dk'_x dk'_y}{4 dK_x dK_y df_s} \sum_{\mathbf{k},s,\mathbf{k}'} \frac{(\sigma+\sigma')^2}{\sigma'^2} R_a(\mathbf{K})^2 \rho_a^2 |D_z(\mathbf{k},+,\mathbf{k}',+)|^2 E(k_x,k_y) E(k'_x,k'_y) \tag{S122}$$

Taking the limit to continuous sums and using a change of variable from (k_x, k_y, k'_x, k'_y) to (f_s, φ, K_x, K_y), with $K_x = k_x + k'_x$, $K_y = k_y + k'_y$ and $f_s = (\sqrt{gk} + \sqrt{gk'})/(2\pi)$ the Jacobian of the coordinate

transform is

$$\det\left(\frac{\partial f_s \partial\varphi \partial K_x \partial K_y}{\partial k_x \partial k_y \partial k'_x \partial k'_y}\right) = \begin{vmatrix} g\cos\varphi/(4\pi\sigma) & -\sin\varphi/k & 1 & 0 \\ g\sin\varphi/(4\pi\sigma) & \cos\varphi/k & 0 & 1 \\ g\cos\varphi'/(4\pi\sigma') & 0 & 1 & 0 \\ g\sin\varphi'/(4\pi\sigma') & 0 & 0 & 1 \end{vmatrix} = \frac{g^2}{4\pi\sigma^3\sigma'}\left[\sigma' - \sigma\cos\left(\varphi-\varphi'\right)\right], \tag{S123}$$

$$\begin{aligned} \int F_{p,2h}(\mathbf{K}, f_s)\mathrm{d}K_x\mathrm{d}K_y\mathrm{d}f_s &= \rho_a^2 \int \frac{(\sigma+\sigma')^2}{4\sigma'^2}\left|R_a\right|^2\left|D_z\right|^2 E(k_x,k_y)E(k_x,k_y)\mathrm{d}k_x\mathrm{d}k_y\mathrm{d}k'_x\mathrm{d}k'_y \\ &= \rho_a^2 \int \frac{(\sigma+\sigma')^2}{4\sigma'^2}\left|R_a\right|^2\left|D_z\right|^2 \frac{E(k_x,k_y)E(k'_x,k'_y)4\pi\sigma^3\sigma'}{g^2\left[\sigma'-\sigma\cos\left(\varphi-\varphi'\right)\right]}\mathrm{d}f_s\mathrm{d}\varphi\mathrm{d}K_x\mathrm{d}K_y. \end{aligned}$$

To transform the spectra to frequency-direction spectra we use the Jacobian :

$$E(f,\varphi) = \frac{4\pi\sigma^3}{g^2}E(k_x,k_y) \tag{S124}$$

And then obtain :

$$\int F_{p,2h}(\mathbf{K}, f_s)\mathrm{d}K_x\mathrm{d}K_y\mathrm{d}f_s = \frac{1}{2}g^2\rho_a^2\int f_s\frac{(\sigma+\sigma')}{4\sigma'^4}\left|R_a\right|^2\left|D_z\right|^2\frac{E(f,\varphi)E(f',\varphi')}{\left[\sigma'-\sigma\cos\left(\varphi-\varphi'\right)\right]}\mathrm{d}f_s\mathrm{d}\varphi\mathrm{d}K_x\mathrm{d}K_y.$$

Now we use the unicity of the Fourier transform to identify the spectral density in the left and right hand sides and considering $|D_z(\mathbf{k},+,\mathbf{k}',+)| \simeq 2\sigma\sigma'$:

$$F_{p,2h}(\mathbf{K}, f_s) = \frac{1}{2}g^2\rho_a^2 f_s\int_0^{2\pi}\frac{\sigma^2(\sigma+\sigma')}{\sigma'^2}\left|R_a\right|^2\frac{E(f,\varphi)E(f',\varphi')}{\sigma'-\sigma\cos\left(\varphi-\varphi'\right)}\mathrm{d}\varphi. \tag{S125}$$

S6.3 Acoustic energy in the water column

We take the acoustic energy per unit of horizontal surface to be twice the kinetic energy. Considering only $K < \Omega/\alpha_w$, we have

$$E_w = \rho_w\int_{-h}^{0} u^2 + w^2\mathrm{d}z \tag{S126}$$

Now expressing the velocities as a function of the velocity pontential in the water given by eq. (S80)

$$E_w = \rho_w\int_{-h}^{0}\sum\left(K^2+\mu^2\right)W_-^2\left(\frac{1+r}{1-r}\right)^2\cos^2(|\mu|z)\mathrm{d}z \tag{S127}$$

$$= \rho_w\int_{\theta_{a,1}}^{\theta_{a,2}}\left(K^2+|\mu|^2\right)F_{p,2h}(\theta_a,\varphi_2,f_s)\left|\frac{A}{P_{2,h}^+}\frac{W_-}{A}\frac{1+r}{1-r}\right|^2\left(\frac{h}{2}+\frac{\sin 2|\mu|h}{4|\mu|}\right)\mathrm{d}\theta_a\mathrm{d}\varphi_2 \tag{S128}$$

with

$$\left|\frac{W_-}{A}\frac{1+r}{1-r}\right| = \left|\frac{2\nu(1+r)}{\mu\left[\mathrm{i}\sin(|\mu|h)+r\cos(|\mu|h)\right]}\right| \tag{S129}$$

and

$$\left|\frac{A}{P^+_{2,h}}\right| = \frac{1}{(\sigma+\sigma')\rho_a}. \tag{S130}$$

Now, looking at the ratio of the acoustic energy and radiated power for any θ_a and φ_2 we have,

$$Q_{max} = \frac{\Omega E_w}{F_{p,2h}(\theta_a,\varphi_2,f_s)/(\rho_a\alpha_a)} \tag{S131}$$

$$= \Omega\rho_w\rho_a\alpha_a\left(K^2+|\mu|^2\right)\left|\frac{A}{P^+_{2,h}}\frac{W_-}{A}\frac{1+r}{1-r}\right|^2\left(\frac{h}{2}+\frac{\sin 2|\mu|h}{4|\mu|}\right) \tag{S132}$$

$$= \frac{\rho_w\alpha_a}{\rho_a\Omega}\left(K^2+|\mu|^2\right)\left|\frac{W_-}{A}\frac{1+r}{1-r}\right|^2\left(\frac{h}{2}+\frac{\sin 2|\mu|h}{4|\mu|}\right) \tag{S133}$$

References

Ardhuin, F. & Herbers, T. H. C., 2013. Noise generation in the solid earth, oceans and atmosphere, from nonlinear interacting surface gravity waves in finite depth, *J. Fluid Mech.*, **716**, 316–348.

Ardhuin, F., Lavanant, T., Obrebski, M., Marié, L., Royer, J.-Y., d'Eu, J.-F., Howe, B. M., Lukas, R., & Aucan, J., 2013. A numerical model for ocean ultra low frequency noise: wave-generated acoustic-gravity and Rayleigh modes, *J. Acoust. Soc. Amer.*, **134**(4), 3242–3259.

Brekhovskikh, L. M., Goncharov, V. V., Kurtepov, V. M., & Naugolnykh, K. A., 1973. The radiation of infrasound into the atmosphere by surface waves in the ocean, *Izv. Atmos. Ocean. Phys.*, **9**, 899–907 (In the English translation, 511–515.).

Cox, C. S. & Jacobs, D. C., 1989. Cartesian diver observations of double frequency pressure fluctuations in the upper levels of the ocean, *Geophys. Res. Lett.*, **16**(8), 807–810.

Hasselmann, K., 1963. A statistical analysis of the generation of microseisms, *Rev. of Geophys.*, **1**(2), 177–210.

Longuet-Higgins, M. S., 1950. A theory of the origin of microseisms, *Phil. Trans. Roy. Soc. London A*, **243**, 1–35.

Stoneley, R., 1926. The effect of the ocean on Rayleigh waves, *Mon. Not. Roy. Astron. Soc.*, **Geophys. Suppl. 1**, 349–356.

Waxler, R. & Gilbert, K. E., 2006. The radiation of atmospheric microbaroms by ocean waves, *J. Acoust. Soc. Amer.*, **119**, 2651–2664.